# Design and synthesis of donor moieties for donor polymers and non-fullerene acceptors for use in organic solar cells

By
Spencer Bradshaw

Senior Honors Thesis
Department of Chemistry
University of North Carolina at Chapel Hill

April 20th, 2020

Approved:

Wei You, Ph.D., Thesis Advisor

Joanna Atkin, Ph.D., Reader

Todd Austell, Ph.D., Reader

## ABSTRACT

Organic solar cells (OSCs) based on bulk heterojunction (BHJ) design have shown substantial promise in the field of renewable alternative energy because of their numerous advantages over traditional inorganic solar cells. Such benefits include low manufacturing costs, light weight, and potential applications on diverse substrates such as flexible films. Ongoing research into BHJ-OSCs has afforded significant performance improvements in recent decades, but further performance optimizations are required before widespread commercialization of organic photovoltaics becomes realistic. The "active layer" of BHJ-OSCs is comprised of the p-type electron donor polymer and n-type electron acceptor, and prior work has shown that both play a role in device performance; as such, this work comprises the design and synthesis of (1) several electron donating monomers of donor polymers and (2) several electron donating moieties of fused-ring non-fullerene acceptors. The synthesis of three different benzodithiophene-based electron donating monomers is herein described. In addition, the design and attempted synthesis of four different non-fullerene fused-ring acceptors is presented, but synthetic optimizations are necessary before these acceptors are successfully synthesized.

## INTRODUCTION

**Background.** As requirements for alternative energy sources continue to increase, considerable attention has been given to the role that photovoltaics may play in alleviating this ongoing demand. Traditional photovoltaic technologies employ inorganic semiconductors and have made appreciable advancements since the inception of the silicon solar cell in 1954;[1,2] however, several barriers prevent the widescale application of inorganic photovoltaics. Organic solar cells (OSCs) have several intrinsic benefits unavailable to traditional inorganic photovoltaics, such as light weight, relatively low material and manufacturing cost, and the ability to function on

a diverse array of substrates that include flexible surfaces.[3,4] These features allow OSCs to break into promising markets (e.g. stretchable/wearable electronics) that remain largely untouched by traditional photovoltaics.

Organic solar cells are frequently based on a bulk heterojunction (BHJ) structure, where an active absorption layer consists of both a p-type donor material and an n-type acceptor material (**Figure 1A**), because organic materials only have short exciton diffusion lengths.[3–7] Successful current generation requires exciton generation (via photon absorption), migration/diffusion to the donor:acceptor interface, dissociation, and charge transport (**Figure 1B**). Effective solar cells must also avoid charge-carrier recombination, whereby a hole and electron encounter each other and recombine, thereby losing the energy associated with the previously absorbed photon.[5–7] In order to maximize BHJ-OSC performance, careful attention must be paid to both the donor and acceptor components of the heterojunction.

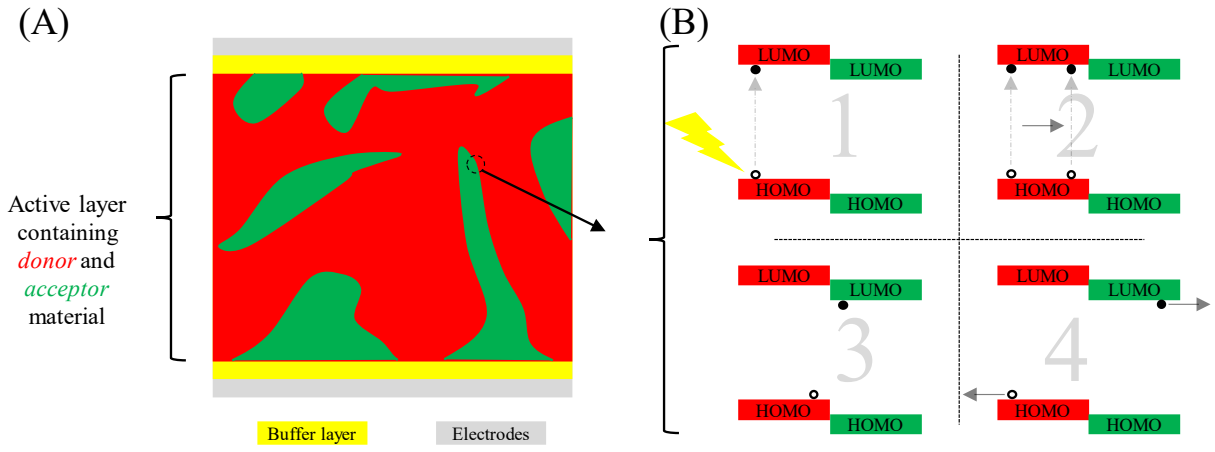


**Figure 1.** General structure and function of a bulk heterojunction organic solar cell. (A) A cross-section of a simplified BHJ OSC. (B) Sequence of events for successful current generation: 1. Absorption of incident light creates excitons; 2. Exciton diffusion to donor-acceptor interface; 3. Exciton dissociation from LUMO of donor material to LUMO of acceptor material; 4. Charge transport through donor and acceptor materials to electrodes. Here a filled circle indicates and electron, and a hollow circle indicates a positive hole. HOMO: highest occupied molecular orbital. LUMO: lowest unoccupied molecular orbital.

**Donor Materials.** While multiple donor materials exist, a prevailing theme within the literature is the use of a conjugated polymer as a donor material. Specifically, the high performance of "-*donor*-linker-*acceptor*-linker-" type co-polymers has made these donor materials increasingly common as this architecture provides excellent electronic tunability. Here, a *donor* unit is an electron rich building block, and an *acceptor* unit is an electron deficient species.[3,8–10] It must be noted, however, that while the polymer has both *donor* and *acceptor* constituents, the resulting polymer is a p-type semiconductor and therefore comprises only half of the active layer. These donor polymers can be broken down into three main constituents (conjugated backbone, oily side chains, and aryl substituents), and it has been shown that the side chains may have a drastic influence on bulk heterojunction morphologies due largely to differential intermolecular interactions and steric considerations.[3,11,12] Our collaborators in the Harald Ade lab at North Carolina State University are interested in understanding how these different side chains can change the packing and organization of the resulting active layer and investigated whether different side chains can induce a change to an ideal morphology. As such, synthesizing three benzo[1,2-b:4,5-b′]dithiophene-based *donor* monomers (**BnDT**, **lin-BnDT**, and **OBnDT**) that differ only in their side chains was selected as an appropriate synthetic target. Construction of photovoltaic devices from these materials may help determine the role that side chains play in donor polymer and overall OSC device performance. While characterizing the performance of OSCs that implement these monomers is the eventual goal, this investigation documents only synthetic procedures and does not include comments on device performance or morphology as this research is still ongoing. **Figure 2** contains a summary of "-*donor*-linker-*acceptor*-linker-" donor materials as well as the chemical structures of the three target *donor* monomers.

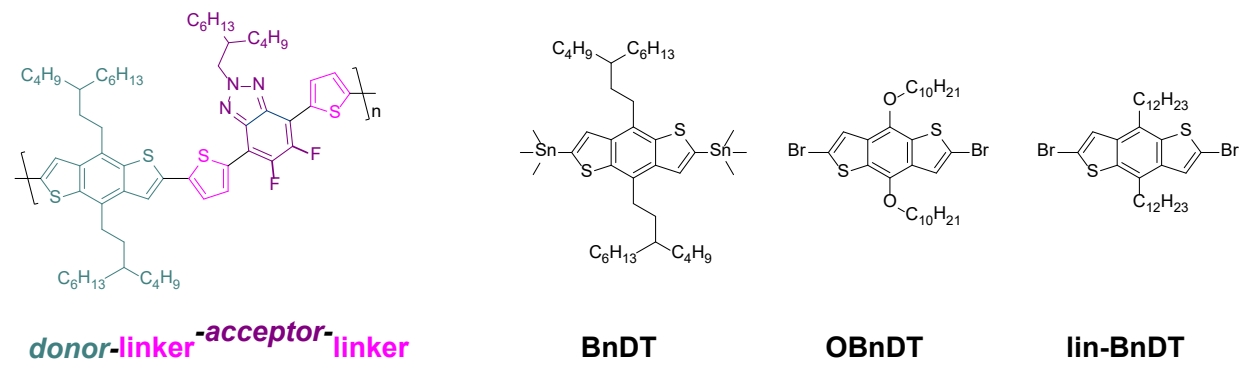


**Figure 2.** Donor used in organic solar cells. (A) Common polymer used as electron donor consisting of electron donating *donor* moiety (here a BnDT monomer), linker, and electron withdrawing *acceptor* moiety (here an FTAZ monomer). (B) Structures of three *donor* monomers whose synthesis is described herein.

**Acceptor Materials.** As with donor materials, there exists a plethora of compounds used as electron acceptors in OSCs. Traditionally, n-type acceptor materials have consisted of derivatized fullerenes, with some of the most common including [6,6]-phenyl-$C_{61}$-butyric acid methyl ester ($PC_{61}BM$) and [6,6]-phenyl-$C_{71}$-butyric acid methyl ester ($PC_{71}BM$).[3,8,13–15] Although the high degree of electron delocalization permits efficient and isotropic electron transport, using fullerene-based acceptors (FAs) presents several drawbacks, including poor absorption in the visible region of the electromagnetic spectrum, restricted electronic tuning abilities, and resource-exhaustive syntheses. While small-molecule non-fullerene acceptors (NFAs) are not without flaws of their own, they have shown promise in recent years, with NFA device performance meeting and even exceeding that of FA devices.[8,13–17] Somewhat analogously to common donor polymers, many NFAs adopt a fused-ring "*acceptor-donor-acceptor*" (A-D-A) structure, with an electron donating core comprised of ~5-13 fused aromatic rings flanked by two electron withdrawing groups. Such acceptors may also be broadly broken down into the same three constituent parts (conjugated backbone, oily side chains, and aryl substituents), and alteration of any of these

constituents results in a concomitant alteration in device performance.[8,13–17] In early 2018, it was shown that steric considerations related to *donor* moiety (A-*D*-A) side chains vastly influence the electronic characteristics of fused-ring small-molecule NFAs.[12] To afford eventual investigation of the role of *donor* moiety side chain steric properties on NFA electronic properties, derivatives of a well-studied indacenodithiophene (IDT) core[18] were designed and set as synthetic targets (**DMIDT**, **M-IDT-A**, **M-IDT-B**). These derivatives differ only by the number of methylene groups in the backbone of the fused-ring core; however, modelling predictions suggest that the steric properties will differ substantially, making these good candidates for later study. Figure 3 contains a summary of fused-ring small-molecule A-D-A acceptor materials as well as the chemical structures of the target *donor* cores.

In addition to designing three IDT-based NFA *donor* cores, this work also discusses the design and synthesis of a new type of NFA after a 2019 publication reported incredibly high performance for an NFA known as Y6.[19] The reported NFA is also based on an A-D-A architecture, but it differs from its more typical NFA counterparts because it contains an internal plane of symmetry and therefore adopts a $C_{2v}$ point group. The unusually high performance observed in devices implementing a Y6 acceptor warrants investigation into other materials that also contain an internal plane of symmetry, so the design of a similar material (**W6**) is presented here.

While all acceptors discussed herein are intended for use in later electronic and photovoltaic experimentation, the contents of this paper related to acceptors, as with donor materials, are strictly related to their design and synthesis, and no device performance is considered.

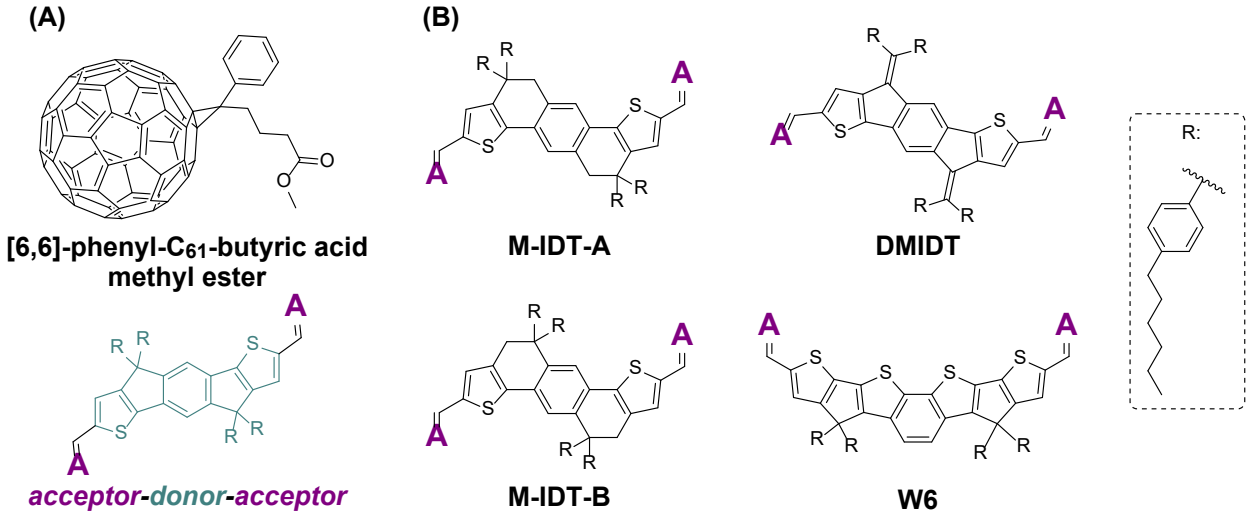


**Figure 3.** Acceptor materials used in organic solar cells. (A) Comparison of common FA to fused-ring small-molecule NFA that contains two *acceptor* moieties flanking a central *donor* moiety (here an IDT core). (B) Structures of all IDT-based donor cores discussed herein. Here, "A" indicates *acceptor* moieties of NFA.

## RESULTS AND DISCUSSION

The synthetic procedures described here are brief and are therefore inexhaustive; for detailed descriptions of procedures, see the included Supplementary Information. In all cases, the presence and purity of a desired product was confirmed by NMR. While NMR spectra are not explicitly discussed within this body of text, as with detailed synthetic procedures, relevant spectra are provided in the Supplementary Information section.

**1. Donor Monomers. BnDT/lin-BnDT.** Synthesis of the **BnDT/lin-BnDT** *donor* monomers may be achieved by a variety of documented means.[20–22] The methods used here are adopted from former You Group member Sam Price and are shown in **Schemes 1 and 2**.[23]

**Scheme 1.** Synthetic route for **BnDT** *donor* monomer synthesis.

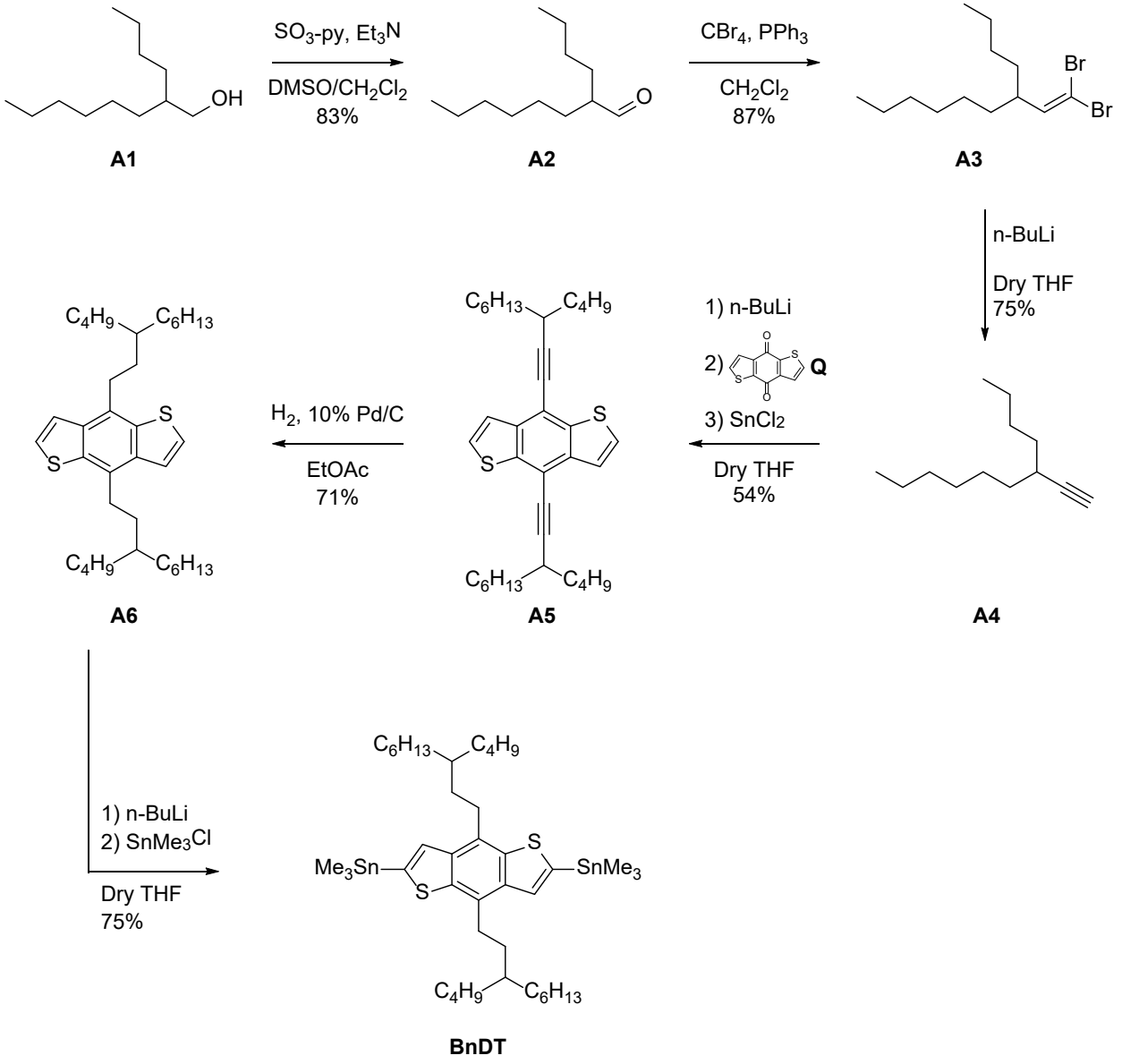


**Scheme 2.** Synthetic route for **lin-BnDT** *donor* monomer synthesis.

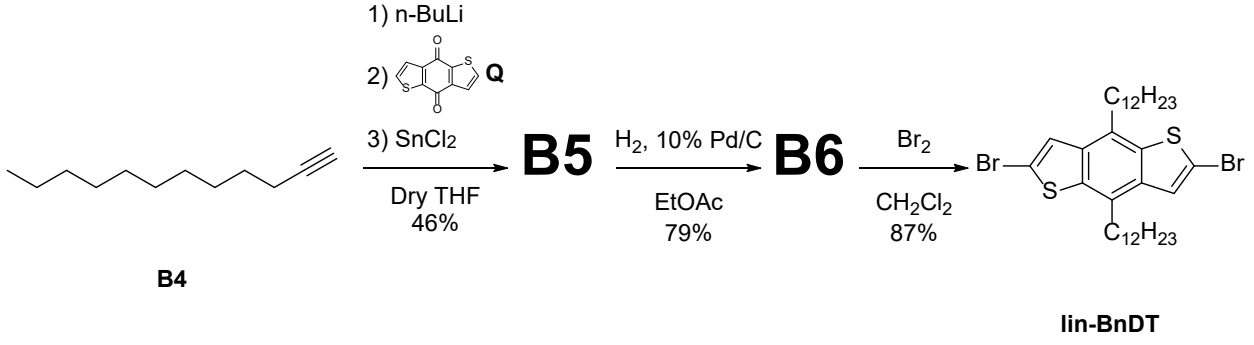

The high-yield oxidation of commercially purchased 2-butyloctanol (**A1**) is accomplished through Parikh-Doering oxidation. Following simple purification, aldehyde **A2** is converted to the alkyne **A4** through a Corey-Fuchs transformation that involves **A3** as the dibromovinyl intermediate. The resultant alkyne **A4/B4** becomes nucleophilic upon lithiation with n-butyllithium and consequently attacks the benzo[1,2-b:4,5-b′]dithiophene quinone (**Q**), which, upon quenching, forms an *in situ* diol (not shown) that undergoes tin(II) mediated reduction[24] to form **A5** or analogous **B5**. This di-alkyne is fully reduced to its corresponding alkane (**A6/B6**) in the presence of hydrogen gas and catalytic palladium on carbon. Finally, **BnDT** is formed following nucleophilic substitution of trimethyltin chloride by lithiated **A6**, and **lin-BnDT** is obtained by brominating **B6** with a solution of bromine dissolved in dichloromethane.

Little to no difficulties were observed in these syntheses, thanks in large part to the procedural optimizations made by Sam Price. However, several important considerations must be noted for successful synthesis to occur. First, while Parikh-Doering oxidation works at room temperature (in contrast to Swern oxidation), it was observed that yields of **A2** were maximized when **A1** was added at 0 °C. Though the exact explanation for this outcome in uncertain, failure to maintain sufficiently low temperature may result in undesirable rearrangement of *in situ* intermediates as is observed in Swern oxidations not kept at or below -78 °C.[25] Also of note is the fact that compound **A3** becomes increasingly dark upon standing for a relatively short period of time (weeks to months); as such, it is important to use this compound as quickly as possible following its isolation. Compounds **A4/B4** seem quite stable over time, though they must be purified to a high degree before lithiation to avoid lithiation byproducts. Vacuum distillation was used to purify **A4/B4**; however, column chromatography might afford increased yields (though at the potential cost of purity, so this alternate purification is difficult to justify). With reference to

synthesis of **A5/B5**, it is critically important to quench the reaction mixture with dilute acid prior to the introduction of tin(II) chloride. Failure to do so will not form the diol necessary for tin(II)-mediated reductive elimination.[24] The necessary introduction of aqueous media to the reaction, however, affords the use of both hydrated and non-hydrated forms of tin(II) chloride, which may make reactions of this type more accessible. Reduction of **A5/B5** to **A6/B6** is straightforward, but care must be taken when working with hydrogen gas due to its flammability and ability to form explosive mixtures in air, even at low concentrations. Also, hydrogen was introduced to the reaction mixture via needle, and there were several occasions throughout the reaction when the flow of hydrogen appeared to stop. Inspection indicated that the palladium catalyst somehow clogged the needle; as a result, the experimenter must be careful to monitor the reaction to fix this issue should it happen to arise. In addition, this reduction requires the use of newer catalyst as older catalyst is often degraded. Transforming **A6** to **BnDT** requires warming the reaction mixture to >0 °C after adding all n-BuLi in order to facilitate lithiation of **A6.** As a final note, the final monomer should not be subjected to column chromatography to prevent unintended removal of the methylated stannyl groups. Recrystallization appears to be the best purification technique, and multiple recrystallization may be done successively to give increasingly pure monomer product. A variety of polar solvents (e.g. methanol, ethanol, isopropanol) are suitable for its recrystallization. Comments on the bromination of **B6** to form **lin-BnDT** are provided below.

**2. Donor Monomers. OBnDT.** Analogs of the **OBnDT** monomer have been synthesized by a large number of researchers.[20,26,27] For perspective, a SciFinder search of a similar compound, differing only in that it has octyloxy side chains (as opposed to decyloxy) results in over 50 distinct publications reporting its synthesis. This is likely due to the limited number of steps needed to

synthesize and purify the final monomer. Although there are multiple ways to synthesize **OBnDT** and its analogs, the most common method (used here) appears in **Scheme 3**.

**Scheme 3.** Synthetic route for **OBnDT** *donor* monomer synthesis.

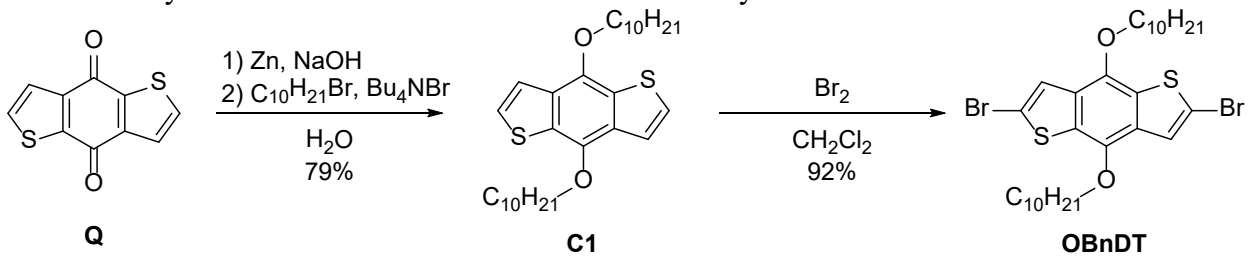


For this synthesis, commercially available quinone **Q** is first exposed to zinc(0) under refluxing (T>110 °C) basic aqueous conditions. Subsequent introduction of an alkyl halide and phase transfer catalyst (e.g. tetrabutylammonium bromide) result in reductive etherification. It is likely that this reaction progresses though a mechanism similar to Williamson etherification followed by reduction to form the aryl ether **C1**.[28] Brominating the resultant product is completed with a solution of elemental bromine in dichloromethane to give the final **OBnDT** monomer.

The well-documented and efficient transformations employed in the synthesis of **OBnDT** mean that this synthesis is neither challenging nor resource exhaustive, so experimenters hoping to carry out similar reactions need only be cognizant of a limited number of factors. In the conversion of **Q** to **C1**, the reaction mixture must vigorously reflux for a minimum of 90 minutes before addition of the alkyl halide and phase transfer catalyst. Insufficient time likely inhibits complete formation of the alkoxy intermediate necessary for Williamson etherification. In addition, vigorous stirring and the presence of a phase-transfer catalyst is vital for the reaction to proceed, for the alkyl halide is otherwise insoluble in aqueous solvent. Alternatively, a less polar solvent could be used, but this would certainly interfere with the dissolution of sodium hydroxide and could hinder reaction progression. Bromination of **C1** with liquid bromine does not result in

over-bromination of the benzodithiophene core, thus helping to maximize the final yield of **OBnDT**; however, experimenters must demonstrate caution when working with the highly volatile and caustic liquid. Dissolving the liquid bromine in an equal volume of solvent helps prevent vaporization of liquid bromine, and dropwise addition of the bromine/dichloromethane solution to a solution of **C1** cooled to 0 ℃ helps to absorb heat from the highly exothermic bromination reaction. Finally, crude mixtures of both **C1** and **OBnDT** tend to be solids, so purification of each compound is efficiently done through recrystallization. This eliminates the need for column chromatography and again aids in maximizing product yield, even though multiple successive recrystallizations were necessary to achieve substantially pure product in both cases. Ethyl and methyl alcohols work well for recrystallizing **C1**, and recrystallization from an alcohol followed by recrystallization from hexanes gave pure product for the final **OBnDT** monomer.

**3. Acceptor Cores. M-IDT-A.** As with the components of donor polymers discussed previously, there are multiple documented ways to synthesize an IDT core. The synthesis presented in **Scheme 4** was designed to incorporate yield-maximizing techniques;[29] unfortunately, the **M-IDT-A** NFA acceptor core was unable to be successfully synthesized. Despite repeated efforts and a wide variety of procedural modifications, little progress was made as even the first necessary transformation was abortive as indicated by NMR (data not shown).

**Scheme 4.** Proposed synthetic route for **M-IDT-A** NFA core.

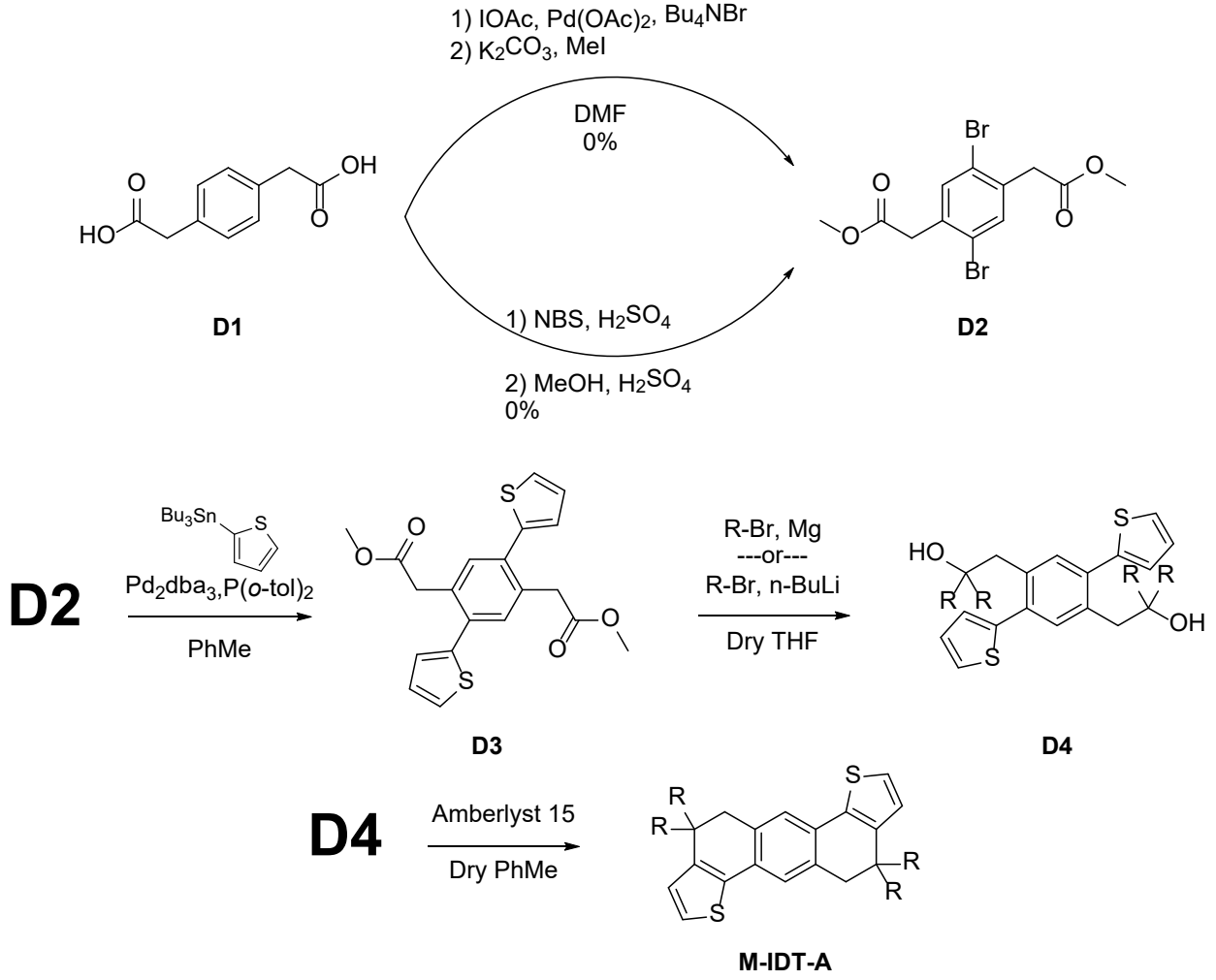


Commercially available **D1** was to undergo tetraalkyl ammonium cation assisted palladium(II)-catalyzed halogenation to form the dibrominated specie **D2.** The viability of this reaction was first shown in 2008, and the same reaction was used in the creation of an NFA in 2018.[30,31] Following halogenation, deprotonation of the carboxylic acid function by a base would enable the dicarboxylate to perform nucleophilic substitution on methyl iodide, thereby converting the dicarboxylic acid into a diester and yielding **D2**. A Stille Coupling would form **D3**, which could then be attacked by a total of four equivalents of nucleophilic side chain (either Grignard or

lithiated) to form **D4**. Amberlyst15 catalyst would facilitate the final reaction to form a ring-closed core, thus forming **M-IDT-A**.

While several factors could have negated the conversion of **D1** to **D2** by tetraalkyl ammonium cation assisted palladium(II)-catalyzed halogenation, the most likely culprit is the presence of the methylene group present between the benzene core and carboxylic acid functional groups on **D1**. The proposed mechanism of this palladium(II) catalysis requires that the carboxylic acid groups be in close proximity to the benzene core to eventually form an intermediate with a five-membered ring composed of the benzene core, carboxylic acid carbonyl carbon, the deprotonated carboxylic acid oxygen, and palladium(II).[30] The extra methylene group could easily prevent the formation of this ring; significant bond angle strain is necessary to allow the palladium(II) to coordinate both the carboxylic acid and ortho position of the benzene ring. Interestingly, NMR analysis also indicated that virtually no esterification was completed. Possible explanations for this are also numerous, but inadequate nucleophilicity of carboxylate groups may play a role.[32]

As the first attempt to synthesize **D2** from **D1** failed, an alternate approach was adopted. One paper reports successful bromination of **D1** using N-bromosuccinimide (NBS) in strongly acidic conditions.[33] This bromination could be followed by Fischer esterification to produce **D2** and allow for the eventual synthesis of **M-IDT-A**. However, more than 5 separate attempts to reproduce this selective bromination were fruitless, and exposure to elemental bromine resulted in no reaction. The reason for these failed reactions remains to be seen, though it is commonly understood that elemental halogens will not add to aromatic compounds in the absence of a Lewis acid.[32]

A final attempt was made to produce a halogenated **D2** using sodium periodate, elemental iodine, and sulfuric acid.[34] The desired halogenation was again unsuccessful despite numerous attempts. Interestingly, an NMR spectrum of the crude reaction mixture had no peaks in the aromatic region, despite full dissolution of the rection mixture into deuterated DMSO. Explanations for this are unknown.

Effective transformation of **D1** to **D2** remains to be observed; perhaps employing Friedel-Crafts halogenation (i.e. elemental bromine and Lewis-acidic iron(III) bromide or aluminum bromide) is the next step in attempting the conversion of **D1** to **D2**.

**4. Acceptor Cores. M-IDT-B.** While the syntheses of **M-IDT-B** and **M-IDT-A** have some similarities, **Scheme 5** demonstrates the proposed synthesis of **M-IDT-B**. As their names might suggest, **M-IDT-B** and **M-IDT-A** are isomers that differ by the location of the methylene groups and side chains. The design of **M-IDT-B** is due in part to the continued inability to make progress in synthesizing **M-IDT-A**.

**Scheme 5.** Proposed synthetic route for **M-IDT-B** NFA core.

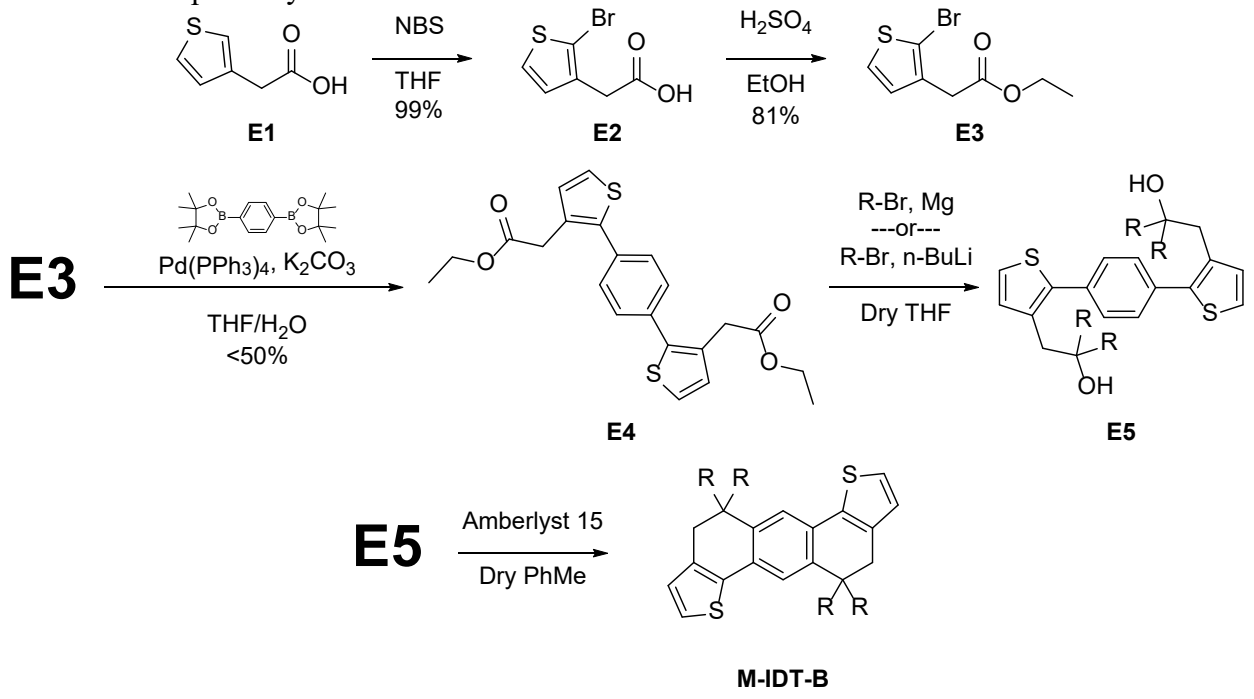

Bromination of 3-thiopheneacetic acid (**E1**) affords 2-bromo-3-thiopheneacetic acid (**E2**), and Fischer esterification of **E2** with ethanol gives the corresponding ethyl ester (**E3**). Suzuki coupling combines two equivalents of **E3** with one equivalent of the commercially purchased 1,4-benzenediboronic acid bis(pinacol) ester to yield **E4**. At this point, the remainder of the synthesis mirrors the final two steps in synthesizing **M-IDT-A**.

With reference to the first reaction (**E1** to **E2**), it is worth noting that a slight excess of NBS was needed to ensure bromination of all **E1** starting material. However, using too much NBS resulted in over-bromination of the substrate. Both byproducts were difficult to remove from the desired mono-brominated product, thus making this reaction challenging. Temperature needed to be kept at 0 °C for at least the first four hours of the reaction to help minimize the risk of over-brominating any **E1**. Following this, it was important to allow the reaction to warm to room temperature and continue stirring overnight. Unfortunately, neither column chromatography nor recrystallization from ethanol yielded entirely pure **E2** product, thus explaining the incredibly high yield. Avoiding this reaction where possible is advisable. Even still, an attempt was made to continue despite having impure **E2**. Esterification of **E2** was best performed as a solvolysis reaction in ethanol; however, methanol would also be a suitable substitute. Minimal concentrated sulfuric acid was needed (5-6 drops per 250 mL), and the reaction needed to be allowed to react for an extended duration (overnight) to ensure completion. Both silica-gel column chromatography and vacuum distillation were used in the attempted purification of **E3**, but it was again impossible to isolate entirely pure **E3**. It should be noted that **E3** is not a solid and therefore cannot be recrystallized.

An unfortunate similarity between both **M-IDT** isomers is their seemingly simple yet practically challenging syntheses. NMR suggests that Suzuki coupling between the benzene

diboronic ester and **E3** was effective, but pure **E4** was again impossible to isolate. Column chromatography proved useless as **E4** consistently precipitated out on the column with each attempted solvent system (hexanes:ethyl acetate from 100:0 to 90:10) despite noting distinct separation when first analyzed via thin layer chromatography. Using a greater percentage of polar solvent resulted in insufficient byproduct separation, and while the reaction mixture could be recovered by flushing the column with a 1:1 mixture of dichloromethane;ethyl acetate, pure **E4** was never eluted. In one instance, precipitation of the mixture on the column resulted in a lab accident when a column exploded after being pressurized. The impurity of **E4** also prevented the successive conversion of **E4** to **E5** even though both Grignard and lithiation procedures were tried (data not shown). As a result, **M-IDT-B** has still not been completely synthesized at this time. Modifications to the procedure including catalyst, solvent, and base have been ineffective at achieving different results.

A Stille coupling between a 2-stannyl version of the 3-thiophene ethyl ester and 1,4-dibromobenzene may allow **E4** to be synthesized and consequently purified, but there are limitations that prevent this approach. First, forming the 2-stannyl 3-thiophene ester would require abstraction of the proton at the 2 position in the thiophene (the bromination reaction would not happen if a Stille coupling were to be used). Such abstraction necessitates the use of a strong base such as n-BuLi or lithium diisopropyl amide (LDA), but n-BuLi is likely to attack the carbonyl of the ester and form a tertiary alcohol upon workup. LDA would likely abstract the alpha-hydrogen of the ester and ultimately form equally disadvantageous products. Thus, while 1,4-dibromobenzene is commercially available, formation of a 2-stannyl-3-thiophene ethyl ester is not probable. Currently, synthesizing **M-IDT-B** appears unlikely.

**5. Acceptor Cores. DMIDT.** One publication reports synthesizing DMIDT, though the authors did not use this material in electron acceptors, and the scheme reported here uses many of the same reactions.[35] Commercially available **F1** undergoes Fischer esterification to form **F2**, which is then coupled with two equivalents of a Stannylated thiophene in **F3**. Saponification reforms the carboxylic acid functional groups seen in **F4**, and a diacyl chloride (**F5**) is formed in nearly stoichiometric yields from oxalyl chloride and catalytic N,N-dimethylformamide. **F5** reacts with Lewis-acidic aluminum trichloride to give **F6** by Friedel-Crafts acylation, and the Wittig reaction seen in Corey-Fuchs transformations gives **F7**. Finally, either Stille or Suzuki coupling allows attachment of the side chains to the core.

**Scheme 6.** Proposed synthetic route for **DMIDT** NFA core.

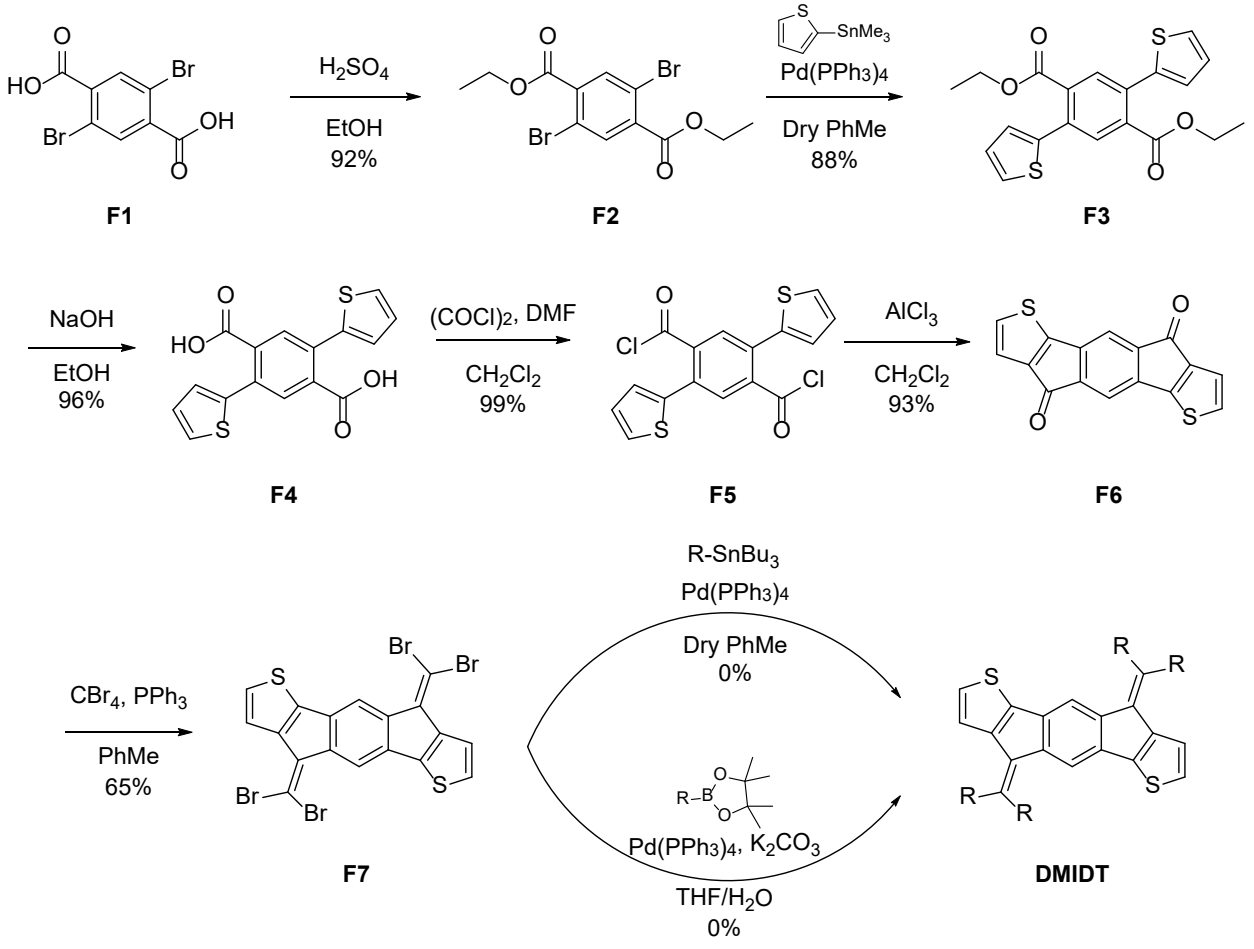

The previous comments on Fischer esterification are again applicable. One must ensure ample reaction time and use the reagent alcohol as the solvent to facilitate total reactivity. In this case, it was observed that leaving the reaction to reflux over the weekend was beneficial for yield of **F2**. For the Stille coupling, palladium(0) was noticeably advantageous when compared to the palladium(II) catalyst that was initially used. Slow degradation of the palladium catalyst in the presence of oxygen meant that quickly establishing and maintaining inert reaction conditions was important, and it was noted that 1:1 hexanes:dichloromethane tended to be the best solvent system for purification of **F3** using silica-gel column chromatography. **F3** was immediately carried to the next transformation, but the white solid could be recrystallized if greater purity is desired. In the synthesis of **F5**, one must be sure to conduct the reaction in an open flask and well-ventilated area, for oxides of carbon are generation throughout the reaction and visible immediately upon the addition of catalytic DMF. This reaction can be left to stir overnight, but the carboxylic acid is insoluble in dichloromethane, so dissolution of all solid means that the reaction may be stopped, concentrated, and the product **F5** carried immediately to the next step without even removing it from the reaction vessel. Friedel-Crafts acylation of **F5** to **F6** is best done at 0 °C with a healthy excess of aluminum chloride (~3.5 equivalents). After full addition of the aluminum chloride, the reaction can warm to room temperature and stir at ambient temperature overnight. Quenching the crude mixture containing **F6** as well as the mixture containing **F7** was best done by pouring into a solution of hydrochloric acid at 0 °C to result in a deep blue (**F6**) or red (**F7**) precipitate. Filtering these products is time consuming, and the products must be oven-dried for several hours in order to remove all water. It is critical to note that neither **F6** nor **F7** are soluble in common NMR solvents. Color, however, is a good indicator of the formation of these products.[35] Further

characterization with mass spectroscopy or elemental analysis is ideal and would have been performed given the luxury of additional time.

At the time of writing, the final **DMIDT** core has not yet been synthesized. The inability for neither Stille nor Suzuki coupling reactions to work thus far is attributed to impure stannylated side chain reactants. Purification of stannylated side chains is difficult as column chromatography will likely remove the trimethyltin moiety entirely, and vacuum distillation is impractical as a result of the side chain's high boiling point. The fact that it is not a solid means that recrystallization is not an option. Suzuki coupling is therefore the most probable way to synthesize **DMIDT** from **F7**. While a Suzuki coupling of this type was unsuccessful in the past, the boronic ester-side chain compound was not purified prior to attempting the Suzuki coupling. Purification of the side chain boronic ester may afford effective Suzuki coupling between the hexylphenyl side chains and **F7**.

**6. Acceptor Cores. W6.** Although a synthetic procedure for **W6** has never been published, many of the reactions instrumental to its production are widely documented.[36–40] Below is the intended scheme through which **W6** will be synthesized as external constraints (i.e. COVID-19) have resulted in incomplete progress.

**Scheme 7.** Proposed synthetic route for **W6** NFA core.

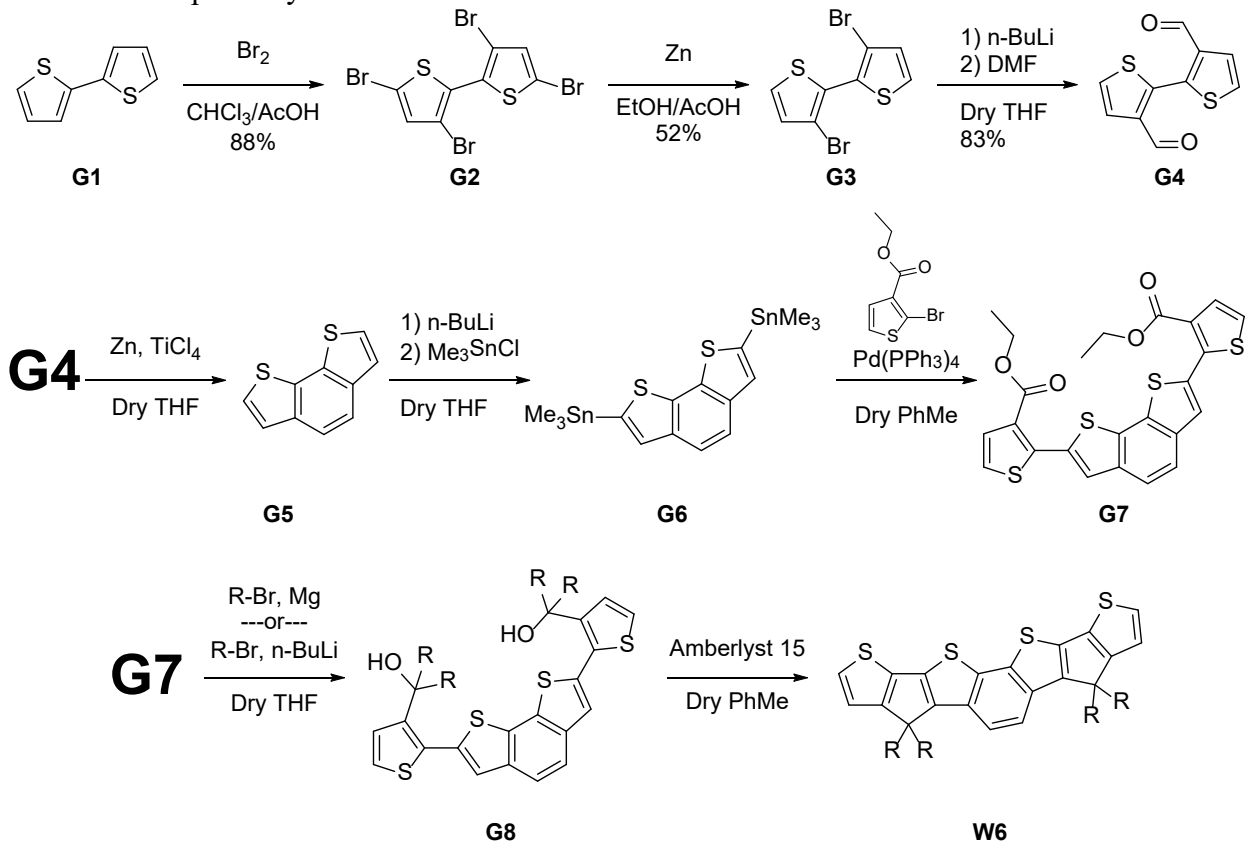


Electrophilic bromination of **G1** with a solution of excess bromine in chloroform forms **G2**, and zinc-mediated reduction removes the halogens at the 5 and 5' positions of **G2** to yield **G3**. Lithiation of **G3** followed by quenching with N,N-dimethylformamide gives the dialdehyde depicted as **G4**, which is then reductively coupled in the presence of zinc and titanium(IV) chloride by the McMurray reaction to give **G5**. Lithiation of the 2 and 2' positions of **G5** followed by nucleophilic substitution of trimethyltin chloride results in **G6**. Palladium-catalyzed Stille coupling is used to attach esterified thiophene units to **G6** to yield **G7**, which is then subject to the same treatment as **D3** and **E4**. **W6** is chemically modified to have a variety of *acceptor* moieties and is then used in OSCs.

Bromination of **G1** with liquid bromine is particularly useful as it affords large scale and efficient synthesis of **G2**, but experimenters must be cautious when working with liquid bromine. Dissolution of the halogen into chloroform is important to prevent its vaporization, as are the temperature and rate of addition of bromine. A temperature of ~0 °C must be maintained while the liquid bromine is added, and the bromine must be added dropwise and over the course of several hours. Ignoring these two necessities creates a safety hazard as the reaction is not only highly exothermic but also produces copious amounts of hydrogen bromide gas. Those attempting to carry out this bromination are advised to do so only in a well-ventilated area as well as to have a steady stream of air flowing over the reaction to be bubbled through a solution of aqueous hydroxide to trap hydrogen bromide gas. In reducing **G2** to **G3**, there are a variety of ways to isolate product, and many publications report different procedures. While filtering and placing the reaction mixture in a cold environment is simple, it also results in low yields. Greater yields could be obtained by removal of the solvent under reduced pressure followed by washing with strong acid (to dissolve zinc) and extraction with an organic solvent such as chloroform. Of critical importance is the order and rate at which reactants are added in the formation of **G4** and **G5**. Lithiation must be done by *slowly* adding **G3** to a mixture of n-BuLi in THF; otherwise, halogen dancing will occur in as a result of the heightened acidity of the 5 and 5' positions of thiophene relative to the 3 and 3' positions.[41] In the reductive coupling reaction that forms **G5**, failure to slowly add **G4** to the mixture of zinc and titanium(IV) chloride results in dimerization and even polymerization of the dialdehyde reactant, thus significantly harming yield. Regrettably, at this time, no further reactions on **Scheme 7** have been completed, though the remaining steps are expected to progress without significant difficulty.

**7. A Note on Palladium-Catalyzed Cross-Coupling Reactions.** While reaction mechanisms are not directly pertinent to the purpose of this manuscript, cross-coupling reactions are key to many of the future polymerizations involving *donor* moieties of donor co-polymers. This type of catalysis is also key to several parts of proposed syntheses for all of the NFA *donor* cores discussed. Both Suzuki and Stille coupling reactions afford formation of carbon-carbon bonds using a palladium-mediated catalytic cycle. In general, they proceed by the same three processes: (I) oxidative addition, (II) transmetalation, and (III) reductive elimination (**Scheme 8**).[42–45] Whereas Stille couplings employ a stannylated species, Suzuki couplings use organoboranes.

**Scheme 8.** General mechanism of Suzuki (A) and Stille (B) cross-coupling reactions.

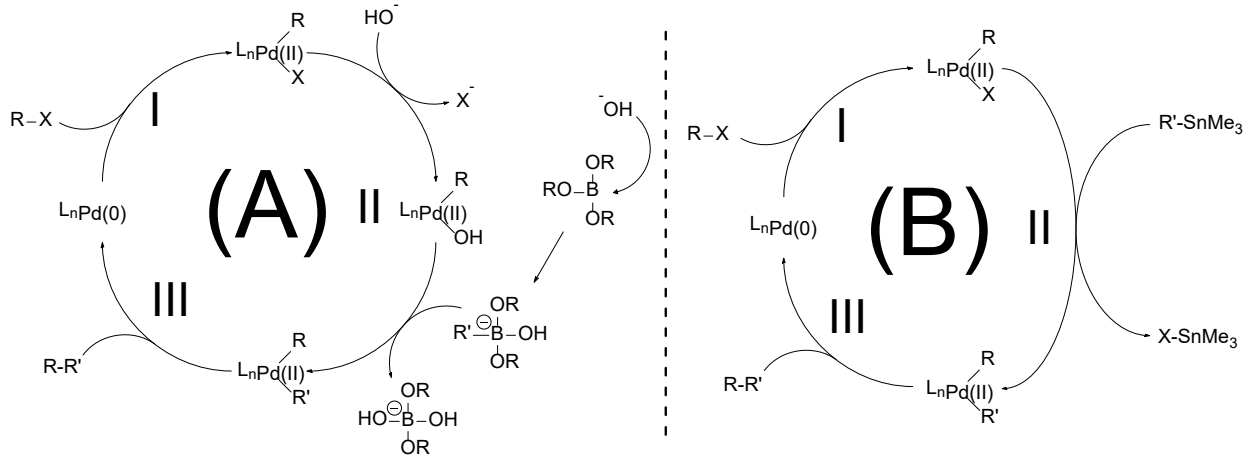


## CONCLUSION

The design and completed or proposed synthesis of three *donor* monomers for donor polymers and four fused-ring *donor* cores for NFAs was presented. As all three benzodithiophene-based *donor* monomers for donor polymers were synthesized with little difficulty, these monomers can be studied to help determine the extent to which *donor* monomer side chain properties alter the performance of organic solar cells employing donor polymers as p-type semiconductors in bulk heterojunction organic solar cells. The robust syntheses suggest that these same synthetic

techniques may also be used to create novel materials for further study of organic solar cells. While synthetic approaches for four different IDT-based NFA *donor* cores are presented, experimental challenges prevented the realization of any of these target cores. As such, synthetic optimizations are necessary before these cores may be examined for their alteration on organic solar cell performance. Ongoing investigation into the various transformations and feasible procedural modifications to enable the production of these *donor* cores is currently underway and will aid in eventual construction and experimentation of these *donor* cores.

## REFERENCES


(1) Chapin, D. M.; Fuller, C. S.; Pearson, G. L. A New Silicon P-n Junction Photocell for Converting Solar Radiation into Electrical Power. *Journal of Applied Physics*. 1954, pp 676–677. https://doi.org/10.1063/1.1721711.

(2) Goetzberger, A.; Hebling, C.; Schock, H.-W. Photovoltaic Materials, History, Status and Outlook. *Mater. Sci. Eng. R Reports* **2003**, *40*, 1–46. https://doi.org/10.1016/S0927-796X(02)00092-X.

(3) Zhou, H.; Yang, L.; You, W. Rational Design of High Performance Conjugated Polymers for Organic Solar Cells. *Macromolecules* **2012**, *45* (2), 607–632. https://doi.org/10.1021/ma201648t.

(4) Ostroverkhova, O. Organic Optoelectronic Materials: Mechanisms and Applications. *Chem. Rev.* **2016**, *116* (22), 13279–13412. https://doi.org/10.1021/acs.chemrev.6b00127.

(5) Sariciftci, N. S.; Smilowitz, L.; Heeger, A. J.; Wudl, F. Photoinduced Electron Transfer from a Conducting Polymer to Buckminsterfullerene. *Science (80-. ).* **1992**, *258* (5087), 1474 LP – 1476. https://doi.org/10.1126/science.258.5087.1474.

(6) Yu, G.; Gao, J.; Hummelen, J. C.; Wudl, F.; Heeger, A. J. Polymer Photovoltaic Cells: Enhanced Efficiencies via a Network of Internal Donor-Acceptor Heterojunctions. *Science (80-. ).* **1995**, *270* (5243), 1789–1791.

(7) Proctor, C. M.; Kuik, M.; Nguyen, T.-Q. Charge Carrier Recombination in Organic Solar Cells. *Prog. Polym. Sci.* **2013**, *38* (12), 1941–1960. https://doi.org/https://doi.org/10.1016/j.progpolymsci.2013.08.008.

(8) Lin, Y.; Zhan, X. Non-Fullerene Acceptors for Organic Photovoltaics: An Emerging Horizon. *Mater. Horizons* **2014**, *1* (5), 470–488. https://doi.org/10.1039/C4MH00042K.

(9) Rech, J. J.; Yan, L.; Peng, Z.; Dai, S.; Zhan, X.; Ade, H.; You, W. Utilizing Difluorinated Thiophene Units To Improve the Performance of Polymer Solar Cells. *Macromolecules* **2019**, *52* (17), 6523–6532. https://doi.org/10.1021/acs.macromol.9b01168.

(10) Abdulrazzaq, O.; Saini, V.; Bourdo, S.; Dervishi, E.; Biris, A. Organic Solar Cells: A Review of Materials, Limitations, and Possibilities for Improvement. *Part. Sci. Technol.* **2013**, *31* (5), 427–442.

(11) Vandewal, K.; Himmelberger, S.; Salleo, A. Structural Factors That Affect the Performance of Organic Bulk Heterojunction Solar Cells. *Macromolecules* **2013**, *46* (16), 6379–6387. https://doi.org/10.1021/ma400924b.

(12) Liu, D.; Yang, L.; Wu, Y.; Wang, X.; Zeng, Y.; Han, G.; Yao, H.; Li, S.; Zhang, S.; Zhang, Y.; Yi, Y.; He, C.; Ma, W.; Hou, J. Tunable Electron Donating and Accepting Properties Achieved by Modulating the Steric Hindrance of Side Chains in A-D-A Small-Molecule Photovoltaic Materials. *Chem. Mater.* **2018**, *30* (3), 619–628. https://doi.org/10.1021/acs.chemmater.7b03142.

(13) Yan, C.; Barlow, S.; Wang, Z.; Yan, H.; Jen, A. K. Y.; Marder, S. R.; Zhan, X. Non-Fullerene Acceptors for Organic Solar Cells. *Nature Reviews Materials*. 2018. https://doi.org/10.1038/natrevmats.2018.3.

(14) Cheng, P.; Li, G.; Zhan, X.; Yang, Y. Next-Generation Organic Photovoltaics Based on Non-Fullerene Acceptors. *Nat. Photonics* **2018**. https://doi.org/10.1038/s41566-018-0104-9.

(15) Wadsworth, A.; Moser, M.; Marks, A.; Little, M. S.; Gasparini, N.; Brabec, C. J.; Baran, D.; McCulloch, I. Critical Review of the Molecular Design Progress in Non-Fullerene Electron Acceptors towards Commercially Viable Organic Solar Cells. *Chemical Society*

*Reviews*. 2019. https://doi.org/10.1039/c7cs00892a.
(16) Zhang, J.; Tan, H. S.; Guo, X.; Facchetti, A.; Yan, H. Material Insights and Challenges for Non-Fullerene Organic Solar Cells Based on Small Molecular Acceptors. *Nat. Energy* **2018**, *3* (9), 720–731. https://doi.org/10.1038/s41560-018-0181-5.
(17) Hou, J.; Inganäs, O.; Friend, R. H.; Gao, F. Organic Solar Cells Based on Non-Fullerene Acceptors. *Nat. Mater.* **2018**, *17* (2), 119–128. https://doi.org/10.1038/nmat5063.
(18) Li, Y.; Gu, M.; Pan, Z.; Zhang, B.; Yang, X.; Gu, J.; Chen, Y. Indacenodithiophene: A Promising Building Block for High Performance Polymer Solar Cells. *J. Mater. Chem. A* **2017**, *5* (22), 10798–10814. https://doi.org/10.1039/C7TA02562A.
(19) Yuan, J.; Zhang, Y.; Zhou, L.; Zhang, G.; Yip, H.-L.; Lau, T.-K.; Lu, X.; Zhu, C.; Peng, H.; Johnson, P. A.; Leclerc, M.; Cao, Y.; Ulanski, J.; Li, Y.; Zou, Y. Single-Junction Organic Solar Cell with over 15% Efficiency Using Fused-Ring Acceptor with Electron-Deficient Core. *Joule* **2019**, *3* (4), 1140–1151. https://doi.org/https://doi.org/10.1016/j.joule.2019.01.004.
(20) Hou, J.; Park, M.-H.; Zhang, S.; Yao, Y.; Chen, L.-M.; Li, J.-H.; Yang, Y. Bandgap and Molecular Energy Level Control of Conjugated Polymer Photovoltaic Materials Based on Benzo[1,2-b:4,5-B′]Dithiophene. *Macromolecules* **2008**, *41* (16), 6012–6018. https://doi.org/10.1021/ma800820r.
(21) Liang, Y.; Feng, D.; Wu, Y.; Tsai, S.-T.; Li, G.; Ray, C.; Yu, L. Highly Efficient Solar Cell Polymers Developed via Fine-Tuning of Structural and Electronic Properties. *J. Am. Chem. Soc.* **2009**, *131* (22), 7792–7799. https://doi.org/10.1021/ja901545q.
(22) Gedefaw, D.; Tessarolo, M.; Zhuang, W.; Kroon, R.; Wang, E.; Bolognesi, M.; Seri, M.; Muccini, M.; Andersson, M. R. Conjugated Polymers Based on Benzodithiophene and Fluorinated Quinoxaline for Bulk Heterojunction Solar Cells: Thiophene versus Thieno[3,2-b]Thiophene as π-Conjugated Spacers. *Polym. Chem.* **2014**, *5* (6), 2083–2093. https://doi.org/10.1039/C3PY01519J.
(23) Price, S. The Synthesis and Optimization of Conjugated Polymers for Photovoltaic Applications, University of North Carolina at Chapel Hill, 2011.
(24) Marshall, J. L.; Lehnherr, D.; Lindner, B. D.; Tykwinski, R. R. Reductive Aromatization/Dearomatization and Elimination Reactions to Access Conjugated Polycyclic Hydrocarbons, Heteroacenes, and Cumulenes. *Chempluschem* **2017**, *82* (7), 967–1001. https://doi.org/10.1002/cplu.201700168.
(25) Tidwell, T. T. Oxidation of Alcohols by Activated Dimethyl Sulfoxide and Related Reactions: An Update. *Synthesis (Stuttg).* **1990**, *1990* (10), 857–870. https://doi.org/10.1055/s-1990-27036.
(26) Pola, M. K.; Boopathi, K. M.; Padhy, H.; Raghunath, P.; Singh, A.; Lin, M.-C.; Chu, C.-W.; Lin, H.-C. Synthesis of Fluorinated Benzotriazole (BTZ)- and Benzodithiophene (BDT)-Based Low-Bandgap Conjugated Polymers for Solar Cell Applications. *Dye. Pigment.* **2017**, *139*, 349–360. https://doi.org/https://doi.org/10.1016/j.dyepig.2016.12.007.
(27) Li, Y.; Xiao, B.; Chen, R.; Chen, H.; Dong, J.; Liu, Y.; Chang, S. Single-Molecule Conductance Investigation of BDT Derivatives: An Additional Pattern Found to Induce through-Space Channels beyond π–π Stacking. *Chem. Commun.* **2019**, *55* (57), 8325–8328. https://doi.org/10.1039/C9CC02998B.
(28) Mandal, S.; Mandal, S.; Ghosh, S. K.; Sar, P.; Ghosh, A.; Saha, R.; Saha, B. A Review on the Advancement of Ether Synthesis from Organic Solvent to Water. *RSC Adv.* **2016**, *6*

(73), 69605–69614. https://doi.org/10.1039/C6RA12914E.
(29) Li, X.; Pan, F.; Sun, C.; Zhang, M.; Wang, Z.; Du, J.; Wang, J.; Xiao, M.; Xue, L.; Zhang, Z.-G.; Zhang, C.; Liu, F.; Li, Y. Simplified Synthetic Routes for Low Cost and High Photovoltaic Performance N-Type Organic Semiconductor Acceptors. *Nat. Commun.* **2019**, *10* (1), 519. https://doi.org/10.1038/s41467-019-08508-3.
(30) Mei, T.-S.; Giri, R.; Maugel, N.; Yu, J.-Q. PdII-Catalyzed Monoselective Ortho Halogenation of C□H Bonds Assisted by Counter Cations: A Complementary Method to Directed Ortho Lithiation. *Angew. Chemie Int. Ed.* **2008**, *47* (28), 5215–5219. https://doi.org/10.1002/anie.200705613.
(31) Zhang, J.; Yan, C.; Wang, W.; Xiao, Y.; Lu, X.; Barlow, S.; Parker, T. C.; Zhan, X.; Marder, S. R. Panchromatic Ternary Photovoltaic Cells Using a Nonfullerene Acceptor Synthesized Using C–H Functionalization. *Chem. Mater.* **2018**, *30* (2), 309–313. https://doi.org/10.1021/acs.chemmater.7b04499.
(32) Bruice, P. Y. Organic Chemistry Bruice. *Org. Chem.* **2004**.
(33) Sarkar, P.; Durola, F.; Bock, H. Dipyreno- and Diperyleno-Anthracenes from Glyoxylic Perkin Reactions. *Chem. Commun.* **2013**, *49* (68), 7552–7554. https://doi.org/10.1039/C3CC44044C.
(34) Koenen, J.-M.; Zhu, X.; Pan, Z.; Feng, F.; Yang, J.; Schanze, K. S. Enhanced Fluorescence Properties of Poly(Phenylene Ethynylene)-Conjugated Polyelectrolytes Designed to Avoid Aggregation. *ACS Macro Lett.* **2014**, *3* (5), 405–409. https://doi.org/10.1021/mz500067k.
(35) Guo, Y.; Li, M.; Zhou, Y.; Song, J.; Bo, Z.; Wang, H. Two-Dimensional Conjugated Polymer Based on Sp2-Carbon Bridged Indacenodithiophene for Efficient Polymer Solar Cells. *Macromolecules* **2017**, *50* (20), 7984–7992. https://doi.org/10.1021/acs.macromol.7b01738.
(36) Beaujuge, P. M.; Tsao, H. N.; Hansen, M. R.; Amb, C. M.; Risko, C.; Subbiah, J.; Choudhury, K. R.; Mavrinskiy, A.; Pisula, W.; Brédas, J.-L.; So, F.; Müllen, K.; Reynolds, J. R. Synthetic Principles Directing Charge Transport in Low-Band-Gap Dithienosilole–Benzothiadiazole Copolymers. *J. Am. Chem. Soc.* **2012**, *134* (21), 8944–8957. https://doi.org/10.1021/ja301898h.
(37) Li, F.; Hu, Z.; Qiao, H.; Liu, L.; Hu, J.; Chen, X.; Li, J. Terpyridine-Based Donor–Acceptor Metallo-Supramolecular Polymers with Tunable Band Gaps: Synthesis and Characterization. *Dye. Pigment.* **2016**, *132*, 142–150. https://doi.org/https://doi.org/10.1016/j.dyepig.2016.04.031.
(38) Oosterhout, S. D.; Savikhin, V.; Zhang, J.; Zhang, Y.; Burgers, M. A.; Marder, S. R.; Bazan, G. C.; Toney, M. F. Mixing Behavior in Small Molecule:Fullerene Organic Photovoltaics. *Chem. Mater.* **2017**, *29* (7), 3062–3069. https://doi.org/10.1021/acs.chemmater.7b00067.
(39) Søndergaard, R.; Manceau, M.; Jørgensen, M.; Krebs, F. C. New Low-Bandgap Materials with Good Stabilities and Efficiencies Comparable to P3HT in R2R-Coated Solar Cells. *Adv. Energy Mater.* **2012**, *2* (4), 415–418. https://doi.org/10.1002/aenm.201100517.
(40) Yoshida, S.; Fujii, M.; Aso, Y.; Otsubo, T.; Ogura, F. Novel Electron Acceptors Bearing a Heteroquinonoid System. 4. Syntheses, Properties, and Charge-Transfer Complexes of 2,7-Bis(Dicyanomethylene)-2,7-Dihydrobenzo[2,1-b:3,4-b']Dithiophene, 2,7-Bis(Dicyanomethylene)-2,7-Dihydrobenzo[1,2-b:4,3-b']Dithiophene,. *J. Org. Chem.* **1994**, *59* (11), 3077–3081. https://doi.org/10.1021/jo00090a027.

(41) Schnürch, M.; Spina, M.; Khan, A. F.; Mihovilovic, M. D.; Stanetty, P. Halogen Dance Reactions—A Review. *Chem. Soc. Rev.* **2007**, *36* (7), 1046–1057. https://doi.org/10.1039/B607701N.
(42) Miyaura, N.; Yamada, K.; Suzuki, A. A New Stereospecific Cross-Coupling by the Palladium-Catalyzed Reaction of 1-Alkenylboranes with 1-Alkenyl or 1-Alkynyl Halides. *Tetrahedron Lett.* **1979**, *20* (36), 3437–3440. https://doi.org/https://doi.org/10.1016/S0040-4039(01)95429-2.
(43) Martin, R.; Buchwald, S. L. Palladium-Catalyzed Suzuki-Miyaura Cross-Coupling Reactions Employing Dialkylbiaryl Phosphine Ligands. *Acc. Chem. Res.* **2008**, *41* (11), 1461–1473. https://doi.org/10.1021/ar800036s.
(44) Matos, K.; Soderquist, J. A. Alkylboranes in the Suzuki−Miyaura Coupling: Stereochemical and Mechanistic Studies. *J. Org. Chem.* **1998**, *63* (3), 461–470. https://doi.org/10.1021/jo971681s.
(45) Espinet, P.; Echavarren, A. M. The Mechanisms of the Stille Reaction. *Angew. Chemie Int. Ed.* **2004**, *43* (36), 4704–4734. https://doi.org/10.1002/anie.200300638.
(46) Hu, Z.; Fu, B.; Aiyar, A.; Reichmanis, E. Synthesis and Characterization of Graft Polymethacrylates Containing Conducting Diphenyldithiophene for Organic Thin-Film Transistors. *J. Polym. Sci. Part A Polym. Chem.* **2012**, *50* (2), 199–206. https://doi.org/10.1002/pola.24957.
(47) Sonntag, M.; Strohriegl, P. Novel Bisindenocarbazole Derivative Exhibiting a Nematic Mesophase. *Tetrahedron Lett.* **2006**, *47* (47), 8313–8317. https://doi.org/https://doi.org/10.1016/j.tetlet.2006.09.089.

# Supplementary Information

**General**

All starting materials were purchased from commercial sources and used without further purification upon receipt. For reactions requiring an inert atmosphere, reaction vessels were evacuated and refilled with argon a minimum of three times. Dry THF was distilled over sodium and benzophenone prior to its use. NMR spectroscopy was performed on a Bruker DRX spectrometer (400 MHz).

**Detailed synthetic procedures**

For chemical structures, see the above text. Exact procedures are provided only for successful reactions.

---

Both **A1 → A2 → A3 → A4 → A5 → A6 → BnDT** and **B4 → B5 → B6** were adapted from the procedures of Sam Price.[23]

Both **Q → C1 → OBnDT** and **B6 → lin-BnDT** were adapted from existing literature procedures.[20,26]

---

**E1 → E2.**

Into an open 250 mL round bottom flask was placed 3-thiopheneacetic acid (**E1**) (10.0 g, 70 mmol, 1 eq). A dry stir bar was added, and the stirring mixture was placed into an ice-water bath to cool to 0 ℃. Once the solution was cooled, NBS (15.0 g, 84 mmol, 1.2 eq) was added, and the temperature was maintained at 0 ℃ for 4 hours. After, the solution was allowed to warm to room

temperature, and it remained stirring for 16 hours. The mixture was then filtered, and the filtrate was concentrated via rotary evaporation. The resulting sludge was dissolved in hexanes and washed with water five times. The organic extracts were dried with magnesium sulfate, filtered, and concentrated. The off-white solid was recrystallized thrice from ethanol for a final yield of 15.3 g (99%) of slightly impure product.

**E2 → E3.**

**E2** (15.0 g, ~ 65 mmol, 1 eq.) was dissolved in ethanol (100 mL) in a 250 mL round bottom flask, and a catalytic amount of concentrated sulfuric acid (5-6 drops) was added. The solution was set to reflux at 95 °C for 18 hours before it was allowed to cool to room temperature. Diethyl ether (50 mL) was added to the solution, and it was washed with saturated sodium carbonate three times. The organic layer was dried with magnesium sulfate, filtered, and concentrated. The dark sludge was purified using a silica gel column using hexanes and ethyl acetate (1:1) and vacuum distillation to give 13.6 g of a yellow oil as product (~80%).

---

**F1 → F2; F3 → F4 → F5 → F6** were conducted according to a previously reported procedure.[35]

**Trimethyl(thiophene-2-yl)stannane**. A stir bar was added to a dry 3-necked round bottom flask, and the flask was evacuated and refilled with argon 5 times. Dry THF (100 mL) was added to the flask via cannula, and thiophene (4 mL, 50 mmol, 1 eq.) was added via syringe. The flask was submerged into a dry ice-acetone bath to cool to -78 °C before n-BuLi (52.5 mmol, 1.05 eq.) was slowly added. The solution stirred for 1 hour. Following, trimethyltin chloride was added to the flask, and the solution continued to stir at -78 °C for 10 minutes. The reaction was allowed to warm to room temperature and stirred for 18 hours. Saturated ammonium chloride (20 mL) was added to quench the reaction before the mixture was poured into diethyl ether (50 mL) and washed with

saturated brine. The organic fraction was dried with magnesium sulfate, filtered, and concentrated. Vacuum distillation afforded 9.3 g of pure clear oil as product (75%).

**F2 → F3.**

**F2** (6.5 g, 17.1 mmol, 1.0 eq.) and trimethyl(thiophene-2-yl)stannane (9.3 g, 17.1 mmol, 2.2 eq.), and $Pd(PPh_3)_4$ were added to a 200 mL round bottom flask, and the flask was evacuated and refilled with argon five times. Dry toluene (75 mL) was added to the flask, and the flask refluxed at 130 °C for 16 hours under an inert atmosphere. The reaction was then poured into 100 mL of water and extracted with diethyl ether five times. The organic fraction was dried, filtered, and concentrated. Silica gel chromatography was used to purify the product using hexanes and dichloromethane (DCM) as eluent for a total yield of 5.8 g (88%).

**F6 → F7.**

A 100 mL round bottom flask was charged with **F6** (0.5 g, 1.7 mmol, 1.0 eq), carbon tetrabromide (2.25 g, 6.79 mmol, 4.0 eq.), and triphenylphosphine (3.56 g, 13.6 mmol, 8.0 eq.). Toluene (30 mL) was added to the flask, and the solution refluxed at 130 °C for 16 hours. The mixture was cooled, poured into a solution of concentrated hydrochloric acid, and filtered with water and dichloromethane for 0.7 g of deep red solid product (65%).

**Tributyl(4-hexylphenyl)stannane** was synthesized according to a reported procedure.[46]

**2-(4-hexylphenyl)-4,4,5,5-tetramethyl-1,3,2-dioxaborolane** was synthesized according to a reported procedure (but was not purified using column chromatography).[47]

---

**G1 → G2.**

2,2'-bithiophene (**G1**) (25 g, 150 mmol, 1.0 eq.) was dissolved in chloroform (270 mL) and acetic acid (135 mL). The solution was cooled to 0 °C before liquid bromine (38.5 mL, 750 mmol, 5.0

eq.) dissolved in an equal volume of chloroform was added slowly over the course of 3 hours. The reaction then stirred for 2 hours at room temperature before finally refluxing for 2 hours. The reaction was cooled, and the solution was poured into methanol (1000 mL) at -35 ℃. The precipitate was collected via filtration, and the product was boiled in ethanol before being cooled to -35 ℃ and filtered. Final yield was 63.4 g (88%).

**G2 → G3.**

**G2** (50 g, 104 mmol, 1.0 eq.) was dissolved in ethanol (250 mL), acetic acid (60 mL), hydrochloric acid (1.5 mL), and water (25 mL). The solution was set to reflux. Zinc dust (32 g, 459 mmol, 4.4 eq.) was added in 3 g portions over the course of 30 minutes, and the reaction continued to reflux for 16 hours after all zinc was added. The reaction was filtered while hot, and the filtrate was cooled to -35 ℃. The yellow precipitate was collected via filtration and recrystallized in hexanes to give 16 g of product (47%).

**G3 → G4.**

A 1 L flask containing a dry stir bar was evacuated and refilled with argon five times. Dry tetrahydrofuran (500 mL) was added, and the flask was placed into a dry ice-acetone bath. Butyllithium (135.5 mmol, 3 eq.) was slowly added to the flask. **G3** (14.6 g, 45.1 mmol, 1.0 eq.) was dissolved in 100 mL dry THF and added dropwise over the course of 2 hours. Once the addition was complete, the solution stirred for another two hours at -78 ℃. N,N-dimethylformamide (12.5 mL, 157.9 mmol, 3.5 eq.) was added to the flask in one portion, and the solution warmed to room temperature. Saturated sodium bicarbonate solution was added to the flask followed by concentrated hydrochloric acid until bubbles started to form, and the THF was removed by rotary evaporation. The solid product was collected by filtration and washed with cold water. Recrystallization from toluene gave 8.4 g (83%) of pure **G4** as product.

**G4 → G5** was performed according to a published procedure.[40]

---

## NMR Spectra

There were no pronounced peaks in spectral regions that have been omitted.

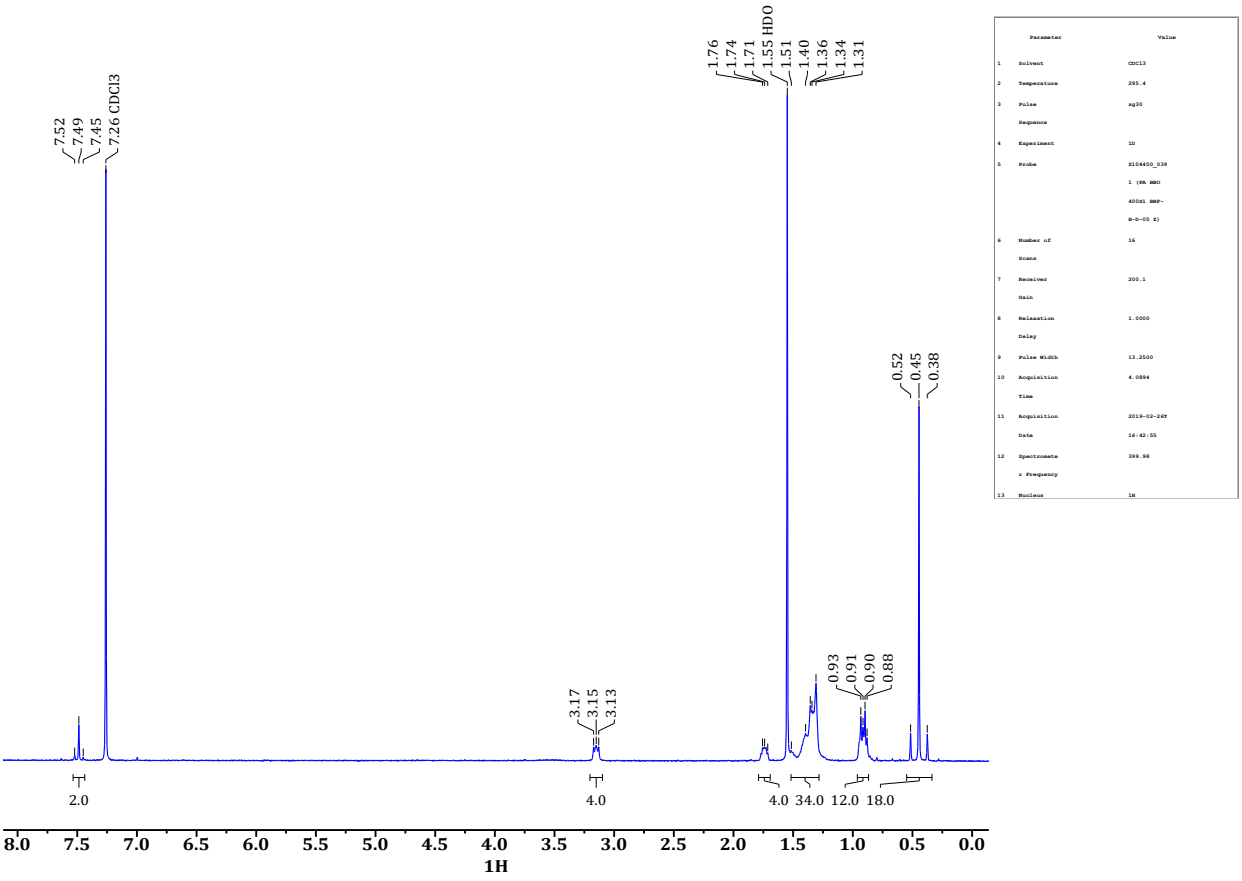


**Figure S1**. $^{1}$H NMR Spectrum for **BnDT**.

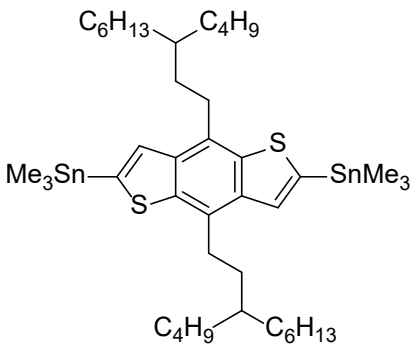

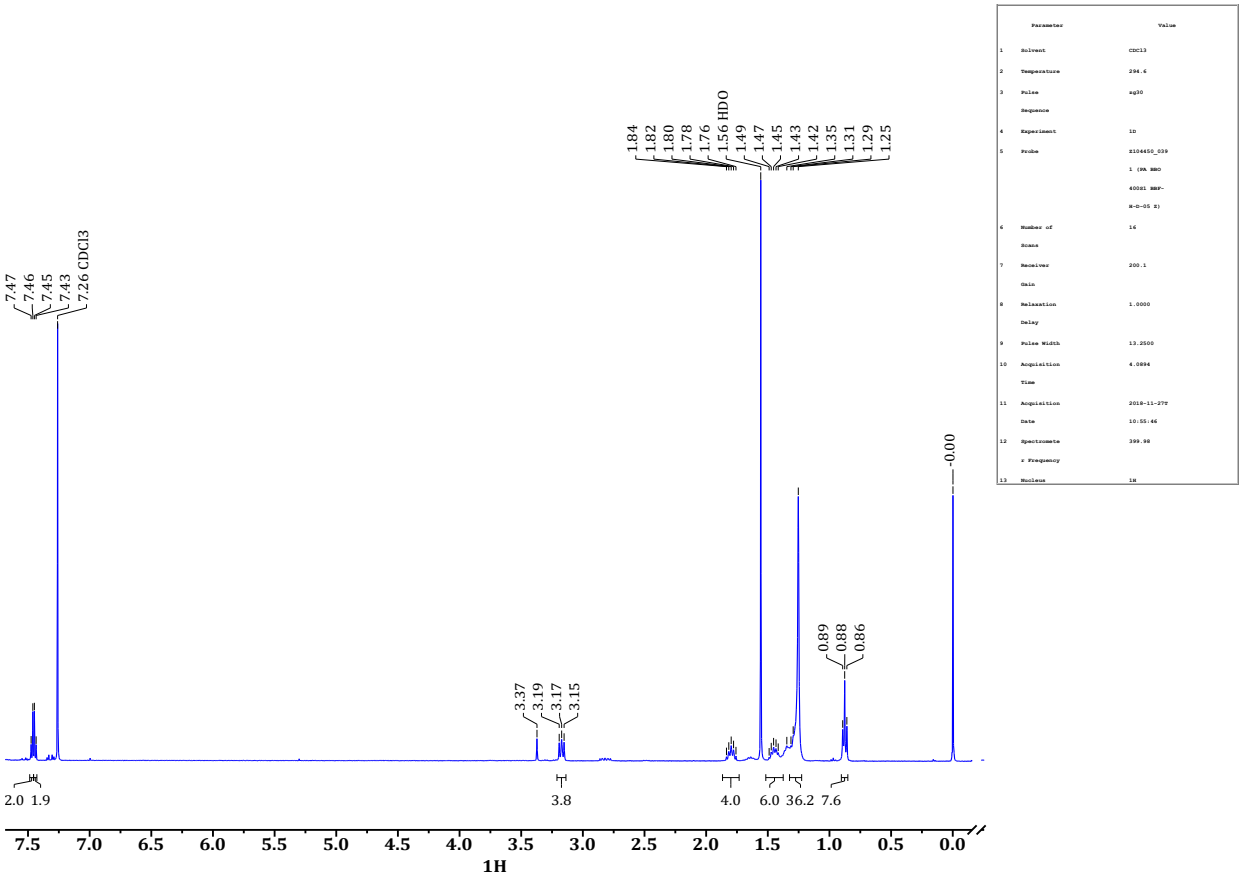


**Figure S2**. $^{1}$H NMR Spectrum for lin-BnDT monomer prior to bromination (**B6**).

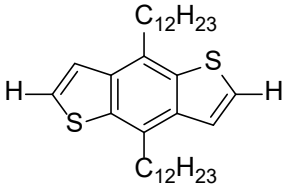

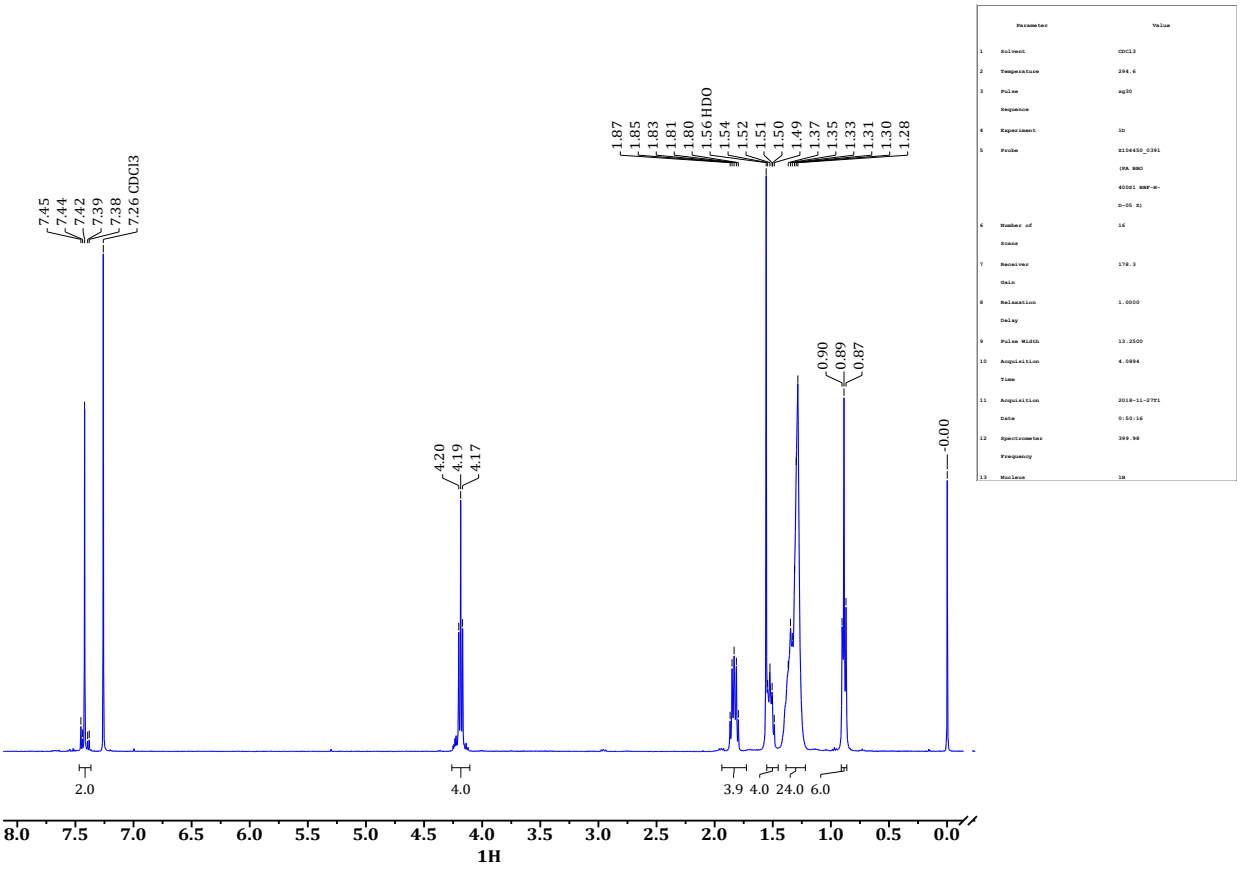


**Figure S3**. $^{1}$H NMR Spectrum for **OBnDT.**

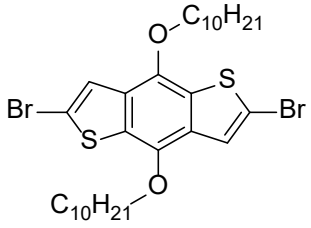

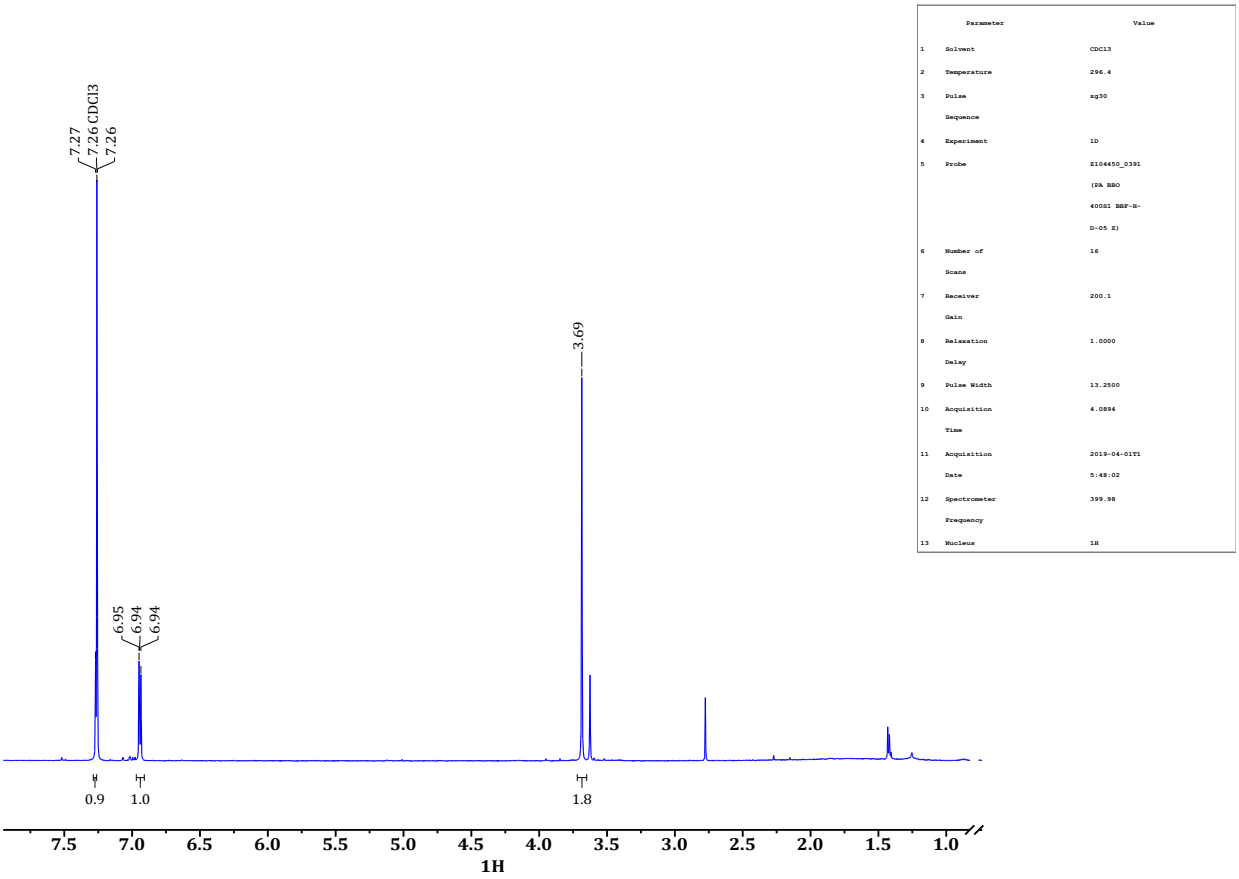


**Figure S4**. $^{1}$H NMR Spectrum for 2-bromo-3-thiopheneacetic acid (**E2**). Note the presence of impurities that were not removed by column chromatography or recrystallization.

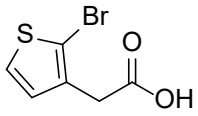

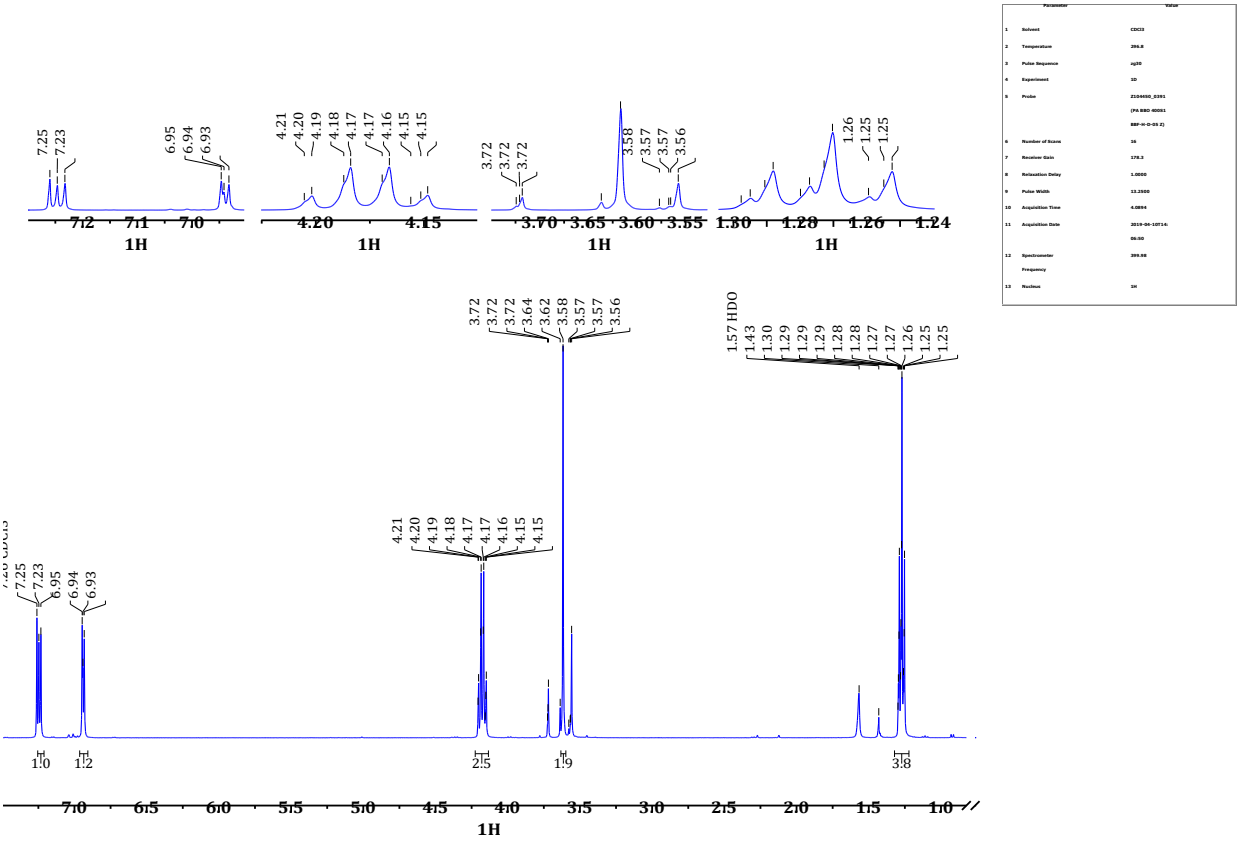

**Figure S5**. $^{1}$H NMR Spectrum for 2-bromo-3-thiopheneacetic acid ethyl ester (**E3**). Note the presence of impurities that were not removed by column chromatography or vacuum distillation.

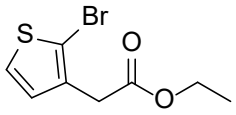

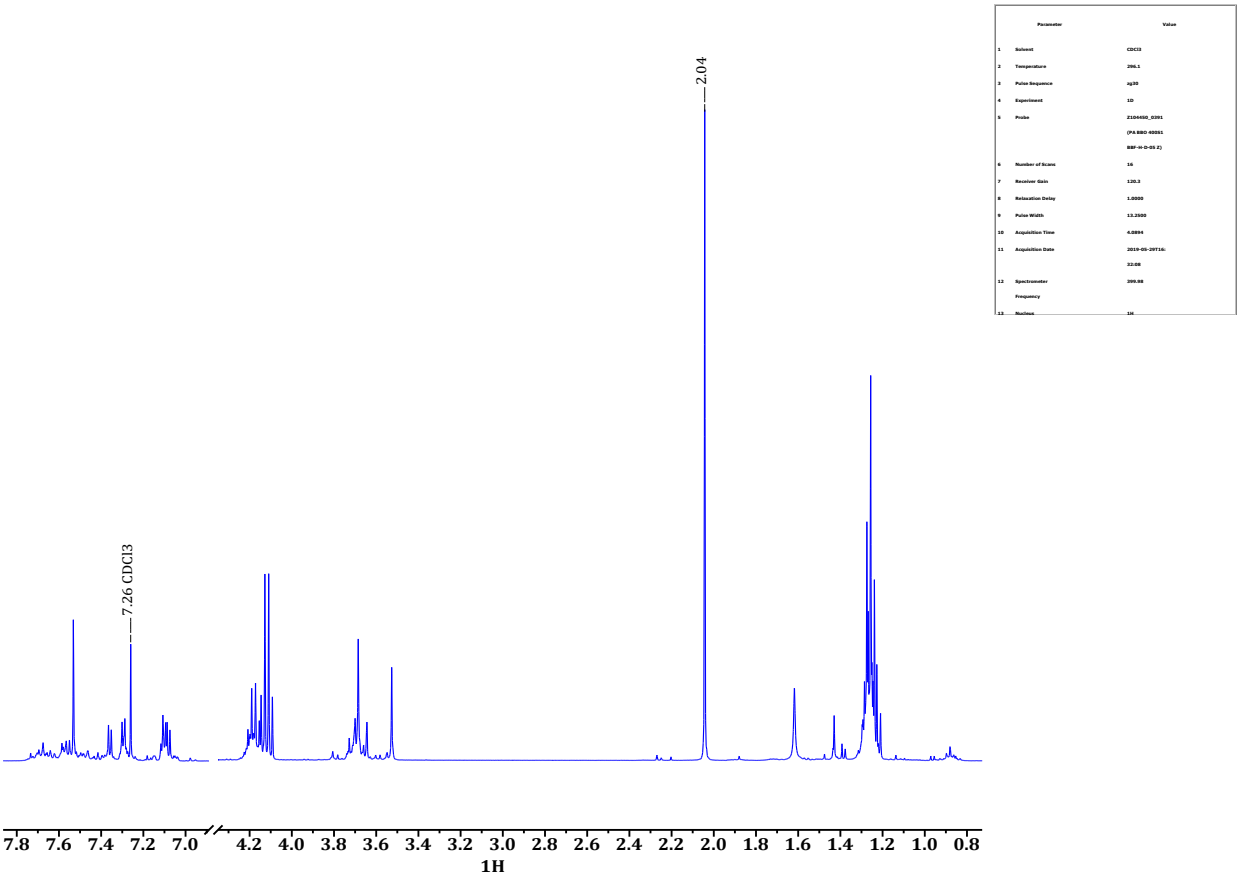


**Figure S6**. $^{1}$H NMR Spectrum for failed Suzuki coupling between **E3** and commercially available 1,4-benzenediboronic acid bis(pinacol) ester to form **E4**. Note the presence of impurities that were not removed by column chromatography.

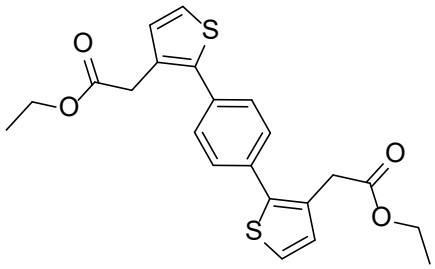

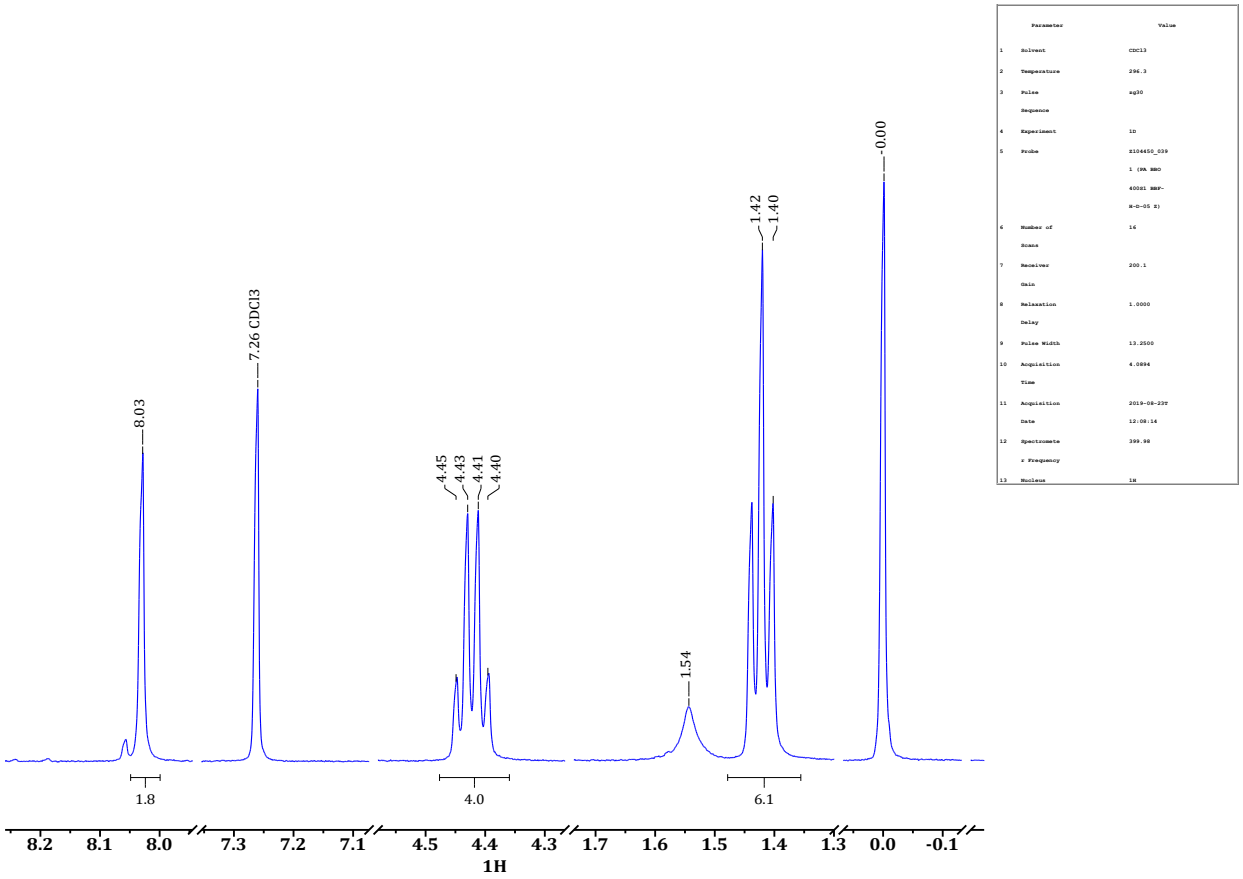


**Figure S7**. $^{1}$H NMR Spectrum for diethyl 2,5-dibromoterephthalate (**F2**).

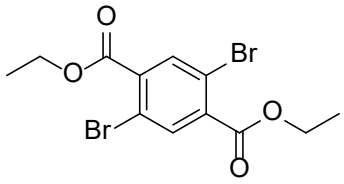

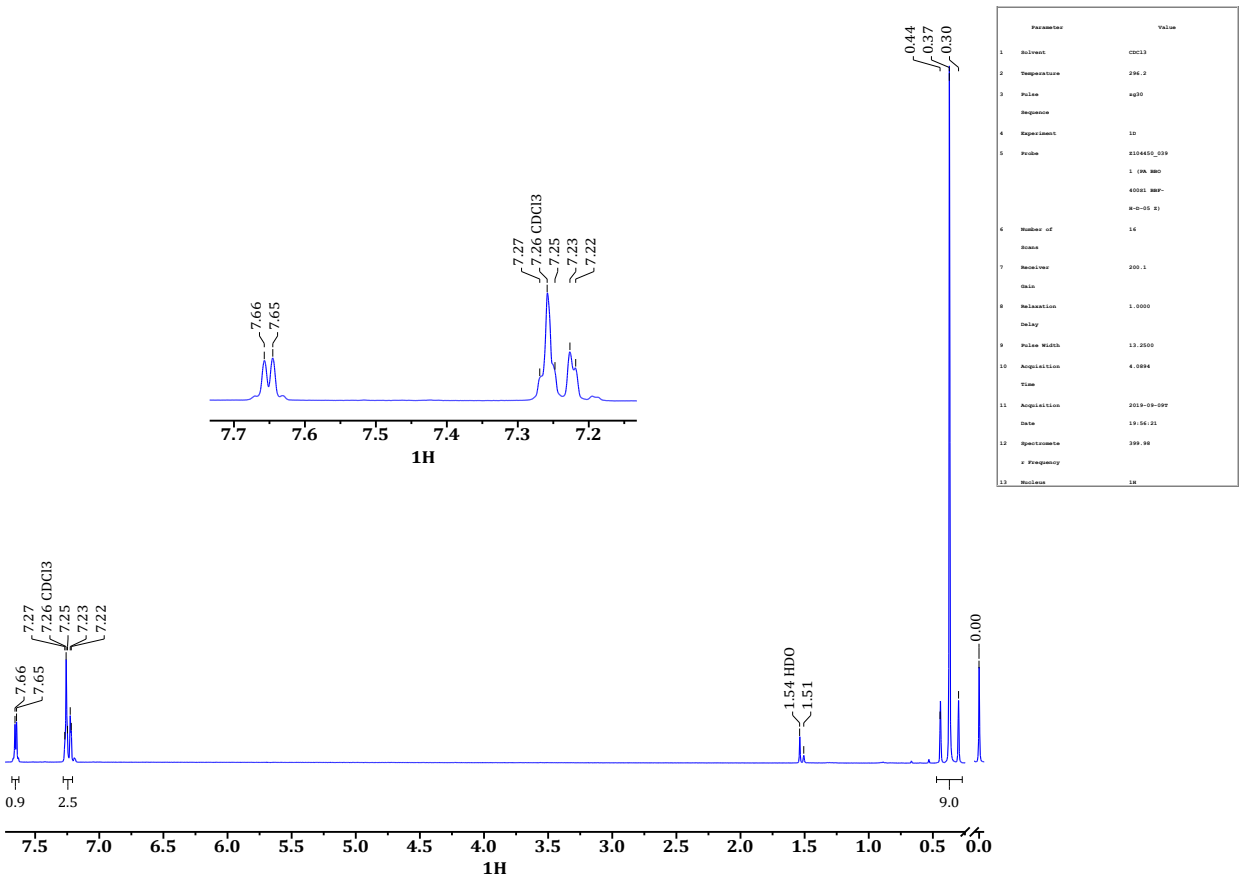


**Figure S8**. $^{1}$H NMR Spectrum for trimethyl(thiophene-2-yl)stannane.

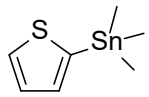

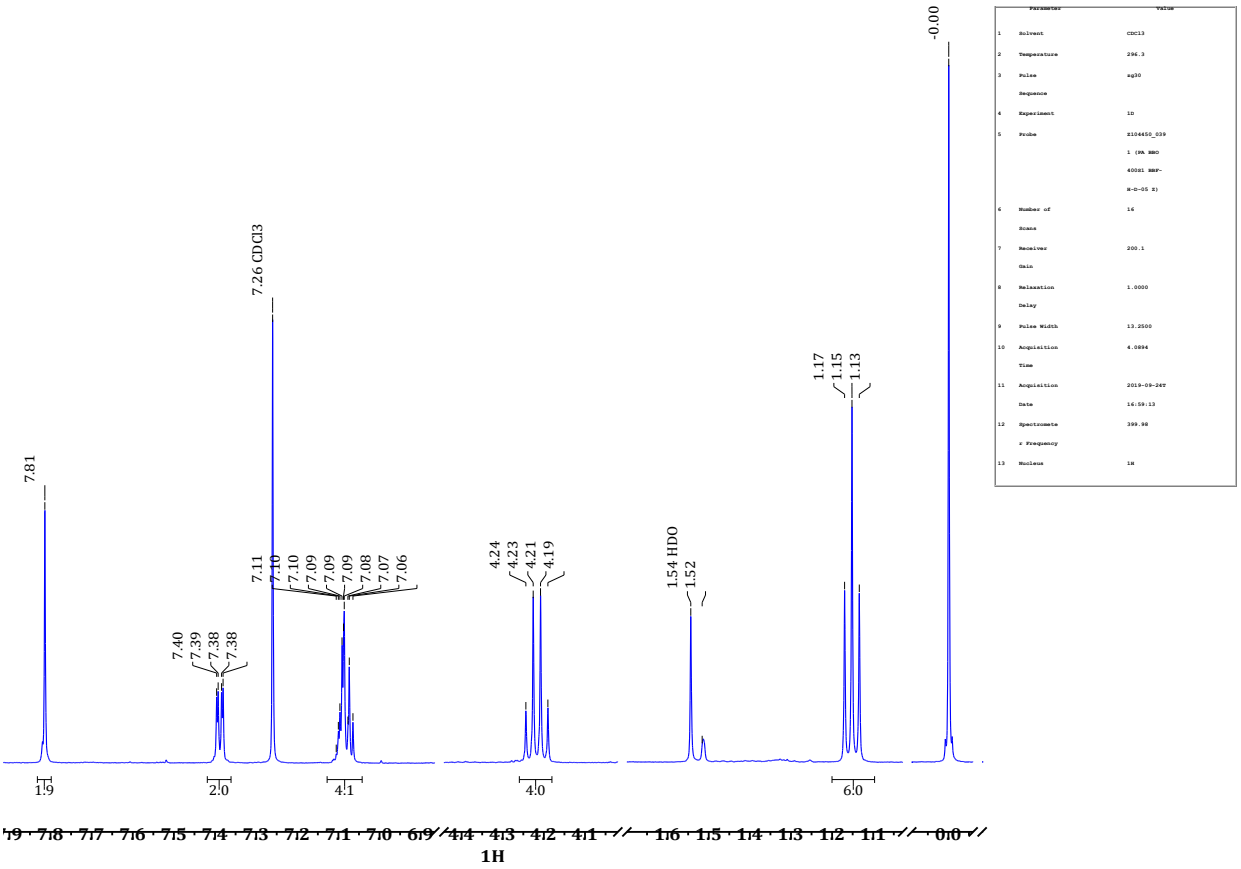


| | Parameter | Value |
|---|---|---|
| 1 | Solvent | CDCl3 |
| 2 | Temperature | 296.3 |
| 3 | Pulse Sequence | zg30 |
| 4 | Experiment | 1D |
| 5 | Probe | Z104450_039 1 (PA BBO 400S1 BBF-H-D-05 Z) |
| 6 | Number of Scans | 16 |
| 7 | Receiver Gain | 200.1 |
| 8 | Relaxation Delay | 1.0000 |
| 9 | Pulse Width | 13.2500 |
| 10 | Acquisition Time | 4.0894 |
| 11 | Acquisition Date | 2019-09-24T 16:59:13 |
| 12 | Spectrometer Frequency | 399.98 |
| 13 | Nucleus | 1H |

**Figure S9**. $^{1}$H NMR Spectrum for diethyl 2,5-di(thiophene-2-yl)terephthalate (**F3**).

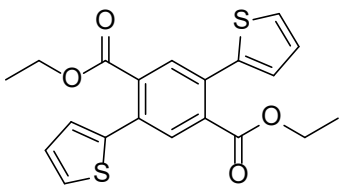

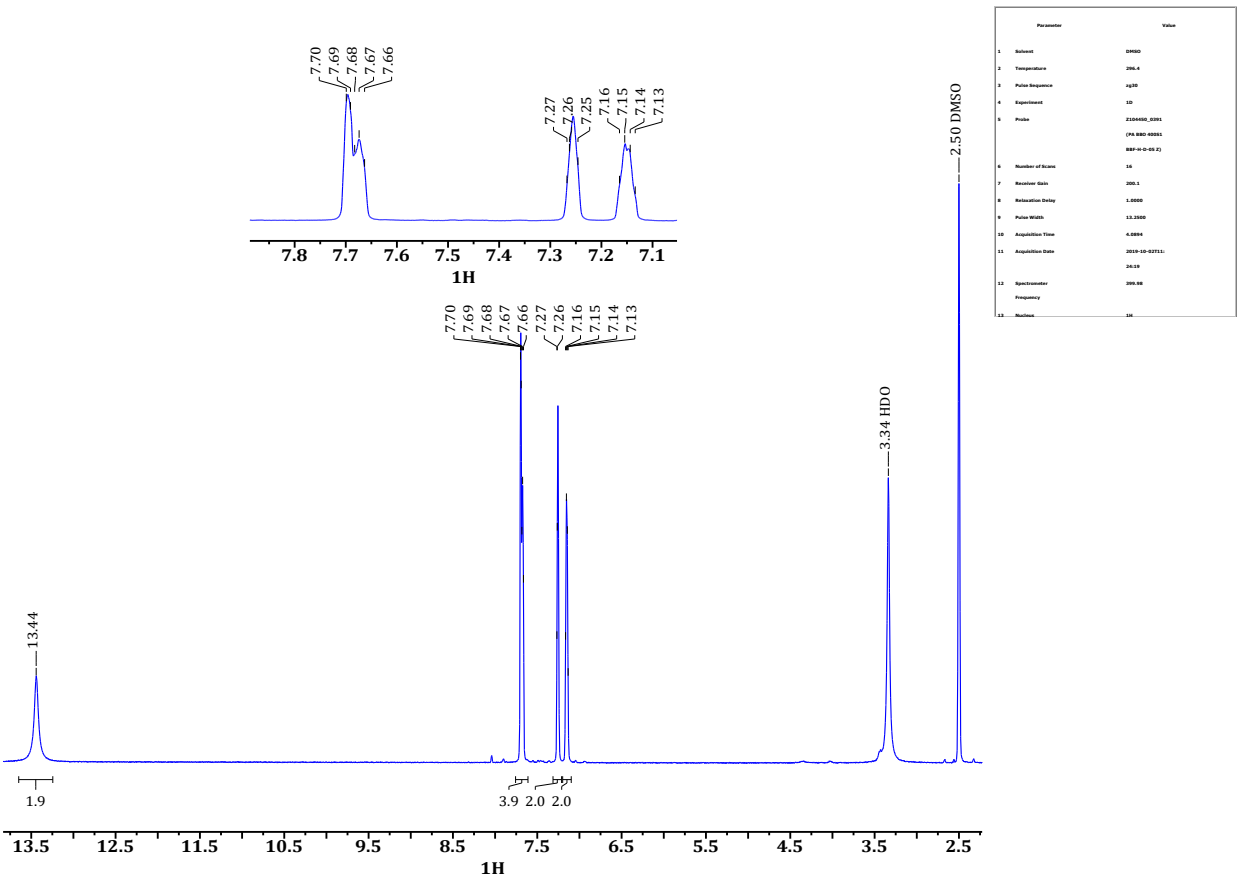


**Figure S10**. $^{1}$H NMR Spectrum for diethyl 2,5-di(thiophene-2-yl)terephthalic acid (**F4**).

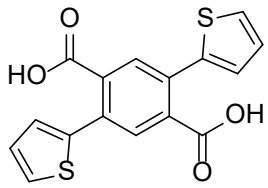

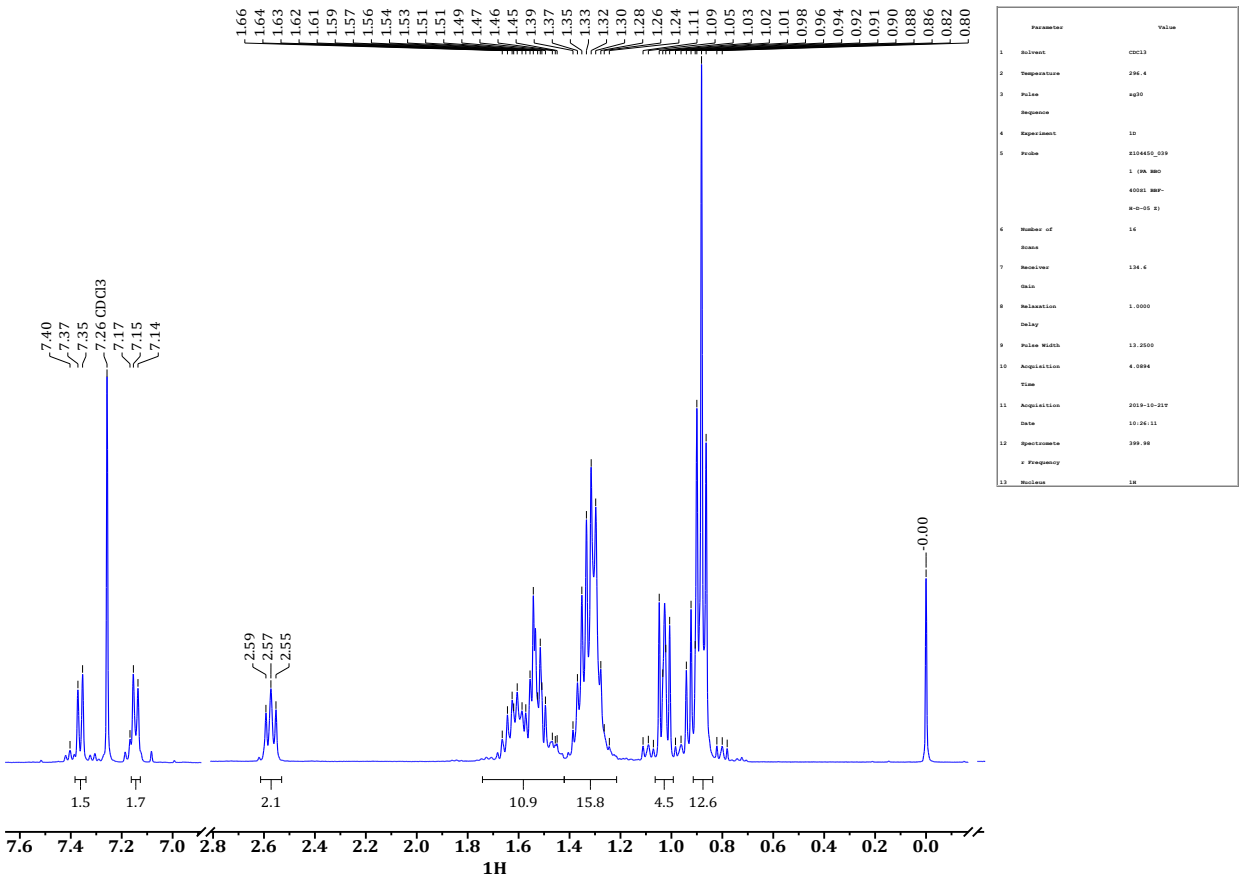


**Figure S11**. $^{1}$H NMR Spectrum for tributyl(4-hexylphenyl)stannane. Note the presence of impurities.

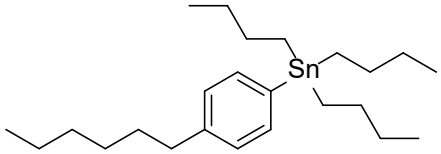

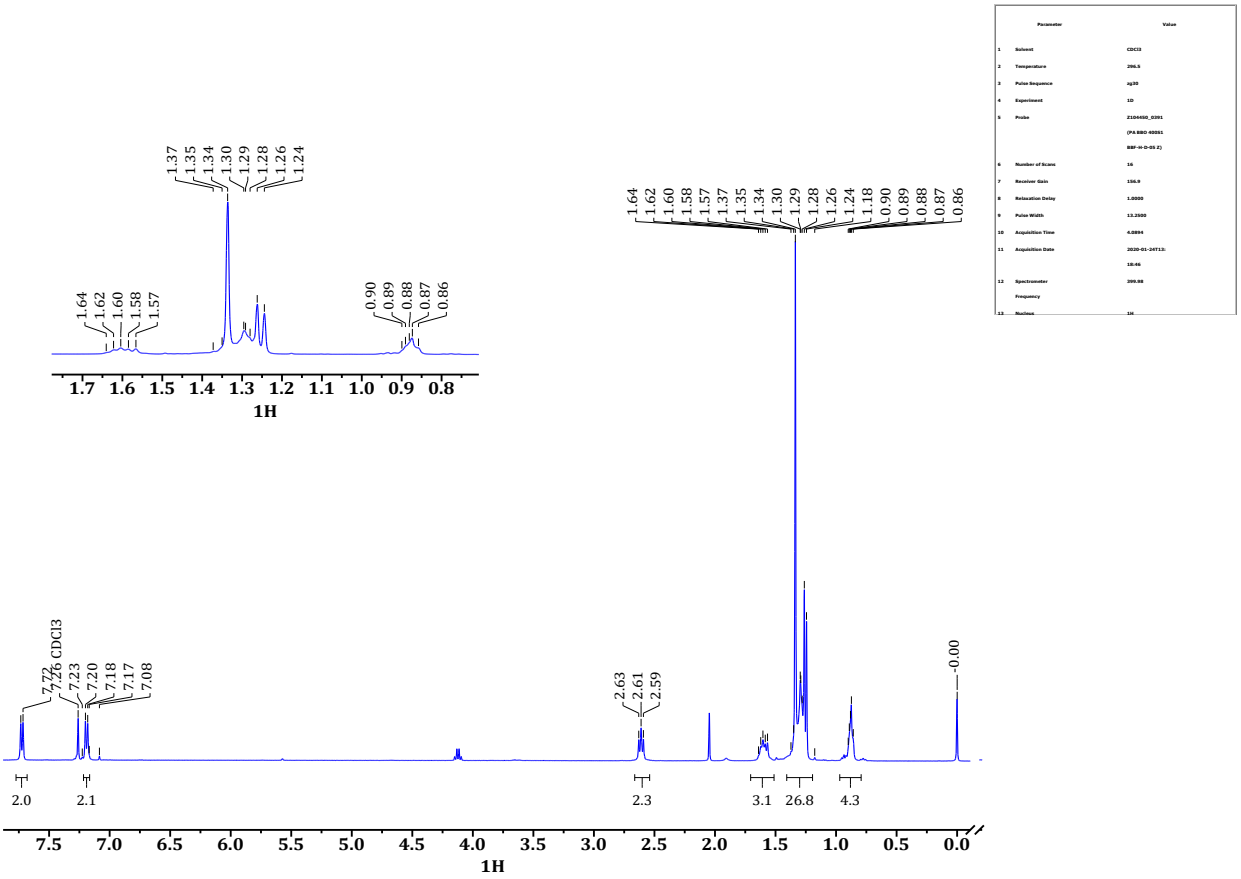


**Figure S12**. $^{1}$H NMR Spectrum for 2-(4-hexylphenyl)-4,4,5,5-tetramethyl-1,3,2-dioxaborolane. Note the presence of impurities.

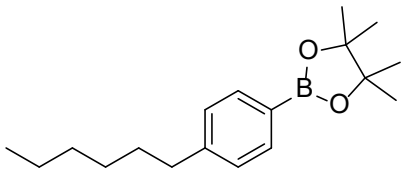

| | Parameter | Value |
|---|---|---|
| 1 | Solvent | CDCl3 |
| 2 | Temperature | 296.1 |
| 3 | Pulse Sequence | zg30 |
| 4 | Experiment | 1D |
| 5 | Probe | S104650_039 1 (PA BBO 400S1 BBF-H-D-05 Z) |
| 6 | Number of Scans | 16 |
| 7 | Receiver Gain | 200.1 |
| 8 | Relaxation Delay | 1.0000 |
| 9 | Pulse Width | 13.7000 |
| 10 | Acquisition Time | 4.0894 |
| 11 | Acquisition Date | 2020-02-14T 16:14:41 |
| 12 | Spectrometer Frequency | 399.98 |
| 13 | Nucleus | 1H |

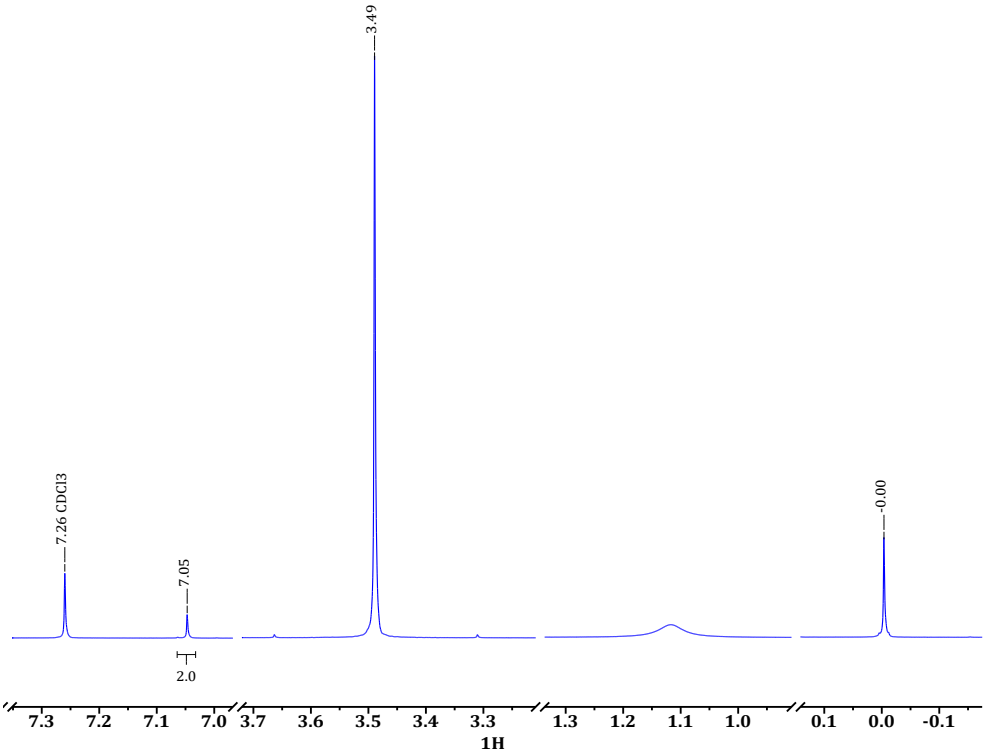


**Figure S13**. $^{1}$H NMR Spectrum 3,3',5,5'-tetrabromo-2,2'-bithiophene (**G2**).

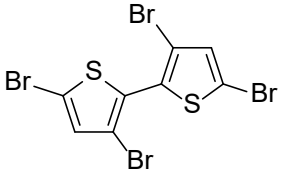

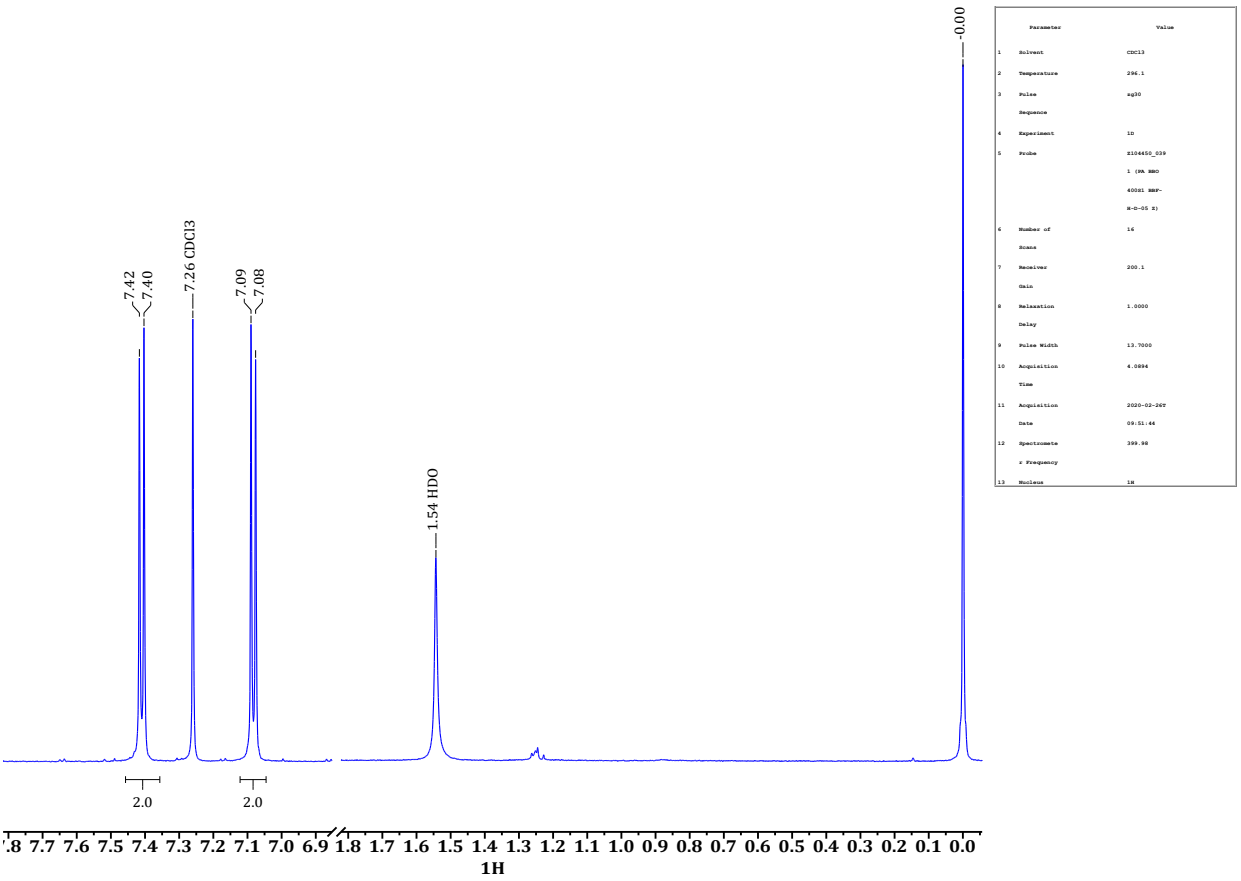


| | Parameter | Value |
|---|---|---|
| 1 | Solvent | CDCl3 |
| 2 | Temperature | 296.1 |
| 3 | Pulse Sequence | zg30 |
| 4 | Experiment | 1D |
| 5 | Probe | S104650_039 1 (PA BBO 400S1 BBF-H-D-05 Z) |
| 6 | Number of Scans | 16 |
| 7 | Receiver Gain | 200.1 |
| 8 | Relaxation Delay | 1.0000 |
| 9 | Pulse Width | 13.7000 |
| 10 | Acquisition Time | 4.0894 |
| 11 | Acquisition Date | 2020-02-26T 09:51:44 |
| 12 | Spectrometer Frequency | 399.98 |
| 13 | Nucleus | 1H |

**Figure S14**. $^{1}$H NMR Spectrum 3,3'-dibromo-2,2'-bithiophene (**G3**).

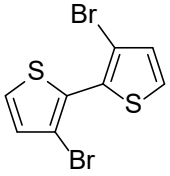

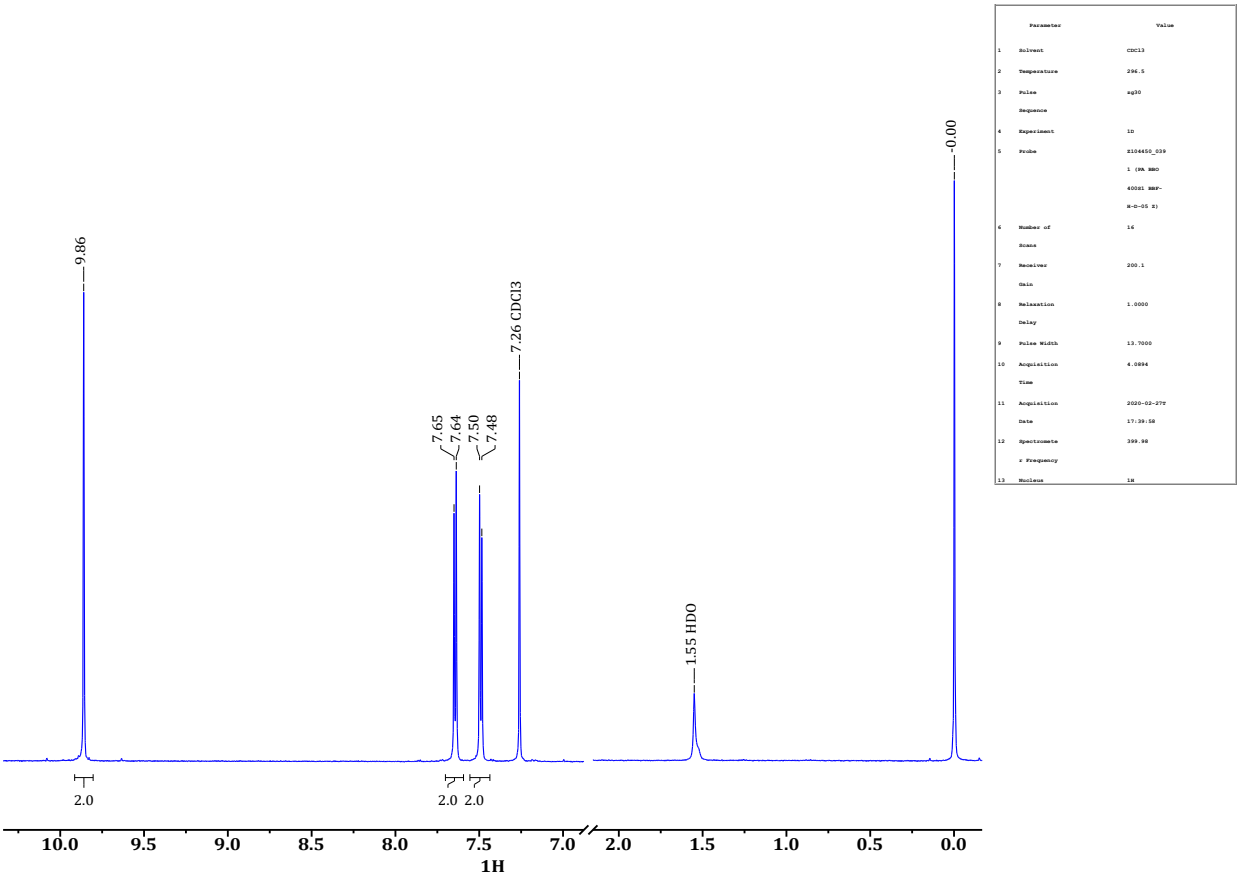


| | Parameter | Value |
|---|---|---|
| 1 | Solvent | CDCl3 |
| 2 | Temperature | 296.5 |
| 3 | Pulse Sequence | zg30 |
| 4 | Experiment | 1D |
| 5 | Probe | S104450_039 1 (PA BBO 400S1 BBF-H-D-05 Z) |
| 6 | Number of Scans | 16 |
| 7 | Receiver Gain | 200.1 |
| 8 | Relaxation Delay | 1.0000 |
| 9 | Pulse Width | 13.7000 |
| 10 | Acquisition Time | 4.0894 |
| 11 | Acquisition Date | 2020-02-27T 17:39:58 |
| 12 | Spectrometer Frequency | 399.98 |
| 13 | Nucleus | 1H |

**Figure S15**. $^{1}$H NMR Spectrum [2,2'-bithiophene]-3,3'-dicarbaldehyde (**G4**).

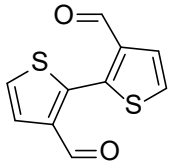

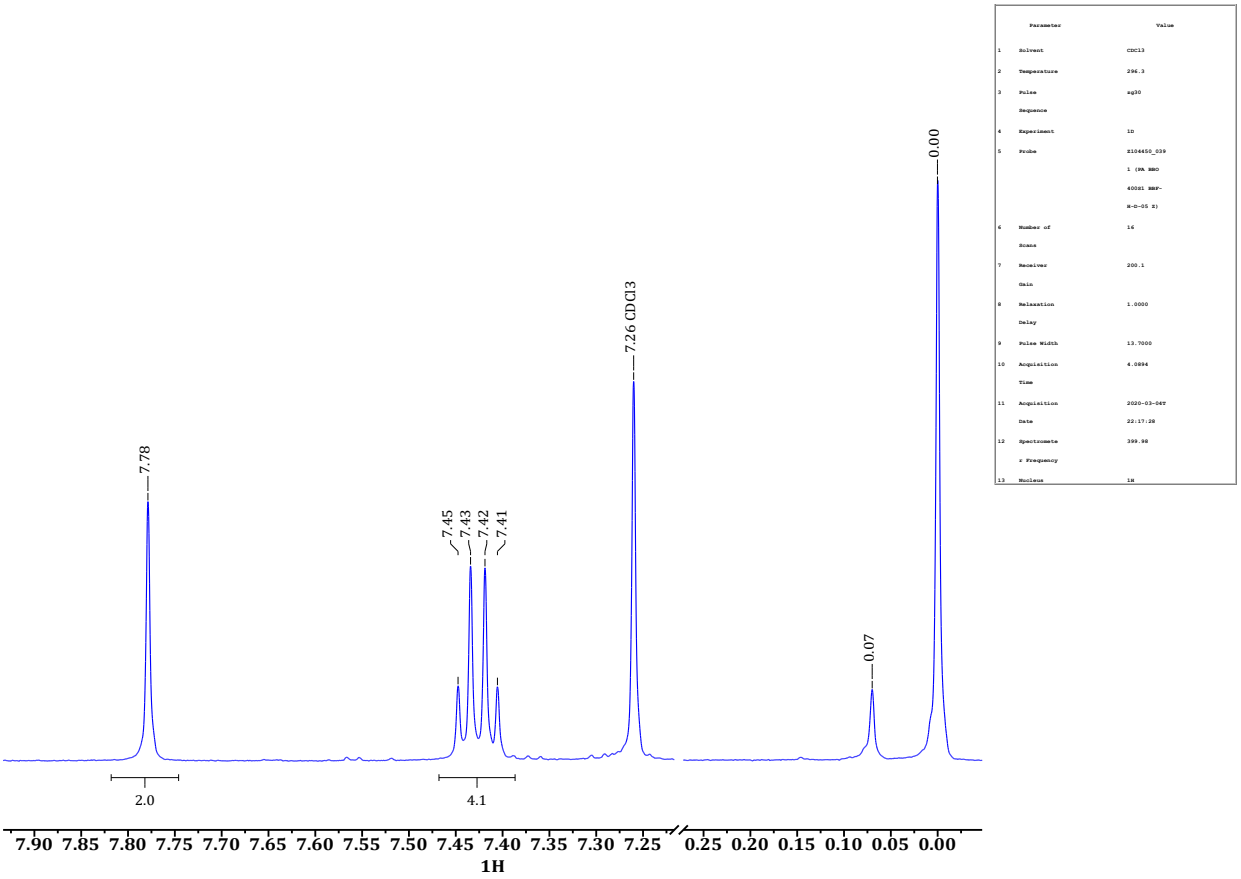


| | Parameter | Value |
|---|---|---|
| 1 | Solvent | CDCl3 |
| 2 | Temperature | 296.3 |
| 3 | Pulse Sequence | zg30 |
| 4 | Experiment | 1D |
| 5 | Probe | S104650_039 1 (PA BBO 400S1 BBF-H-D-05 Z) |
| 6 | Number of Scans | 16 |
| 7 | Receiver Gain | 200.1 |
| 8 | Relaxation Delay | 1.0000 |
| 9 | Pulse Width | 13.7000 |
| 10 | Acquisition Time | 4.0894 |
| 11 | Acquisition Date | 2020-03-04T 22:17:28 |
| 12 | Spectrometer Frequency | 399.98 |
| 13 | Nucleus | 1H |

**Figure S16**. $^{1}$H NMR Spectrum for benzo[2,1-b:3,4-b']dithiophene (**G5**).

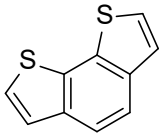

**Miscellaneous Images**


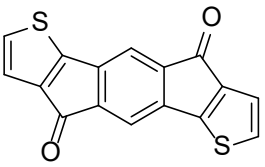


**F6**

**Figure S17.** Filtration of **F6**. Note the deep blue color used to confirm its identity.[35]

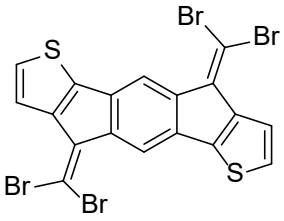


**F7**

**Figure S18.** Appearance of **F7**. Note the red color used to confirm its identity.[35]

**Figure S19**. Recrystallization of 3,3',5,5'-tetrabromo-2,2'-bithiophene (**G2**) from methanol.

**Figure S20.** Needle-like appearance of [2,2'-bithiophene]-3,3'-dicarbaldehyde (**G4**) after recrystallization from toluene.

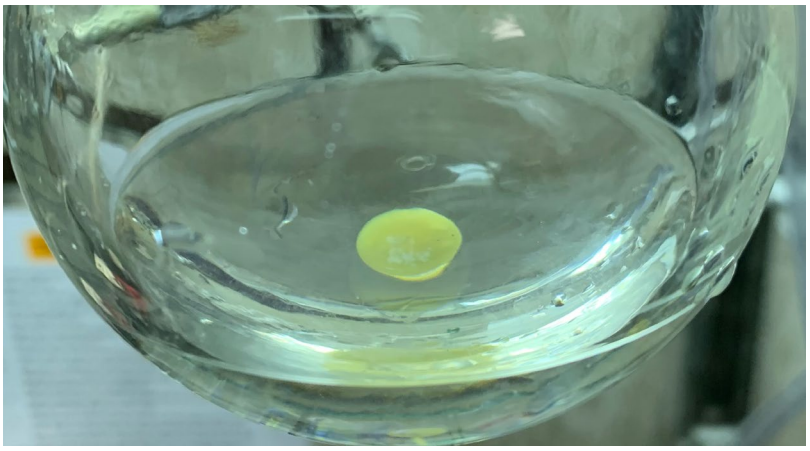

**Figure S21**. Insolubility of benzo[2,1-b:3,4-b']dithiophene (**G5**) in methanol.